





## Article

# Green Synthesis and Molecular Docking Study of Some New Thiazoles Using Terephthalohydrazide Chitosan Hydrogel as Ecofriendly Biopolymeric Catalyst

Jehan Y. Al-Humaidi <sup>1</sup>, Sobhi M. Gomha <sup>2,\*</sup> , Nahed A. Abd El-Ghany <sup>3,\*</sup>, Basant Farag <sup>4</sup>, Magdi E. A. Zaki <sup>5</sup> , Tariq Z. Abolibda <sup>2</sup>  and Nadia A. Mohamed <sup>3,6</sup> 

<sup>1</sup> Department of Chemistry, College of Science, Princess Nourah bint Abdulrahman University, P.O. Box 84428, Riyadh 11671, Saudi Arabia; jyalhamidi@pnu.edu.sa

<sup>2</sup> Department of Chemistry, Faculty of Science, Islamic University of Madinah, P.O. Box 170, Madinah 42351, Saudi Arabia; t.z.a@iu.edu.sa

<sup>3</sup> Department of Chemistry, Faculty of Science, Cairo University, Giza 12613, Egypt; na.ahmed@qu.edu.sa

<sup>4</sup> Department of Chemistry, Faculty of Science, Zagazig University, Zagazig 44519, Egypt; basantfarag@zu.edu.eg

<sup>5</sup> Department of Chemistry, Faculty of Science, Imam Mohammad Ibn Saud Islamic University (IMSIU), P.O. Box 5701, Riyadh 11623, Saudi Arabia; mezaki@imamu.edu.sa

<sup>6</sup> Department of Chemistry, College of Science, Qassim University, P.O. Box 6644, Buraidah 51452, Saudi Arabia

\* Correspondence: smgomha@iu.edu.sa (S.M.G.); abdelghanyn@sci.cu.edu.eg (N.A.A.E.-G.)

**Abstract:** Terephthalohydrazide chitosan hydrogel (TCs) was prepared and investigated as an ecofriendly biopolymeric catalyst for synthesis of some novel thiazole and thiadiazole derivatives. Thus, TCs was used as a promising ecofriendly basic biocatalyst for preparation of three new series of thiazoles and two thiadiazoles derivatives via reacting 2-(2-oxo-1,2-diphenylethylidene) hydrazine-1-carbothio-amide with various hydrazonoyl chlorides and  $\alpha$ -haloketones under mild ultrasonic irradiation. Also, their yield% was estimated using chitosan and TCs in a comparative study. The procedure being employed has the advantages of mild reaction conditions, quick reaction durations, and high reaction yields. It also benefits from the catalyst's capacity to be reused several times without significantly losing potency. The chemical structures of the newly prepared compounds were confirmed by IR, MS, and <sup>1</sup>H-NMR. Docking analyses of the synthesized compounds' binding modes revealed promising binding scores against the various amino acids of the selected protein (PDB Code—1JII). SwissADME's online tool is then used to analyze the physiochemical and pharmacokinetic characteristics of the most significant substances. The majority of novel compounds showed zero violation from Lipinski's rule (Ro5).

**Keywords:** thiosemicarbazones; thiazoles; thiadiazoles; hydrazonoyl halides; antimicrobial; molecular docking studies; in silico ADMET



**Citation:** Al-Humaidi, J.Y.; Gomha, S.M.; El-Ghany, N.A.A.; Farag, B.; Zaki, M.E.A.; Abolibda, T.Z.; Mohamed, N.A. Green Synthesis and Molecular Docking Study of Some New Thiazoles Using Terephthalohydrazide Chitosan Hydrogel as Ecofriendly Biopolymeric Catalyst. *Catalysts* **2023**, *13*, 1311. <https://doi.org/10.3390/catal13091311>

Received: 27 July 2023

Revised: 4 September 2023

Accepted: 8 September 2023

Published: 20 September 2023



**Copyright:** © 2023 by the authors. Licensee MDPI, Basel, Switzerland. This article is an open access article distributed under the terms and conditions of the Creative Commons Attribution (CC BY) license (<https://creativecommons.org/licenses/by/4.0/>).

## 1. Introduction

Green chemistry has received a great deal of attention in recent years due to its potential to lower human risk, reduce environmental pollution, lessen the dangers of chemicals, and eliminate waste. The catalyst is essential in organic synthesis to reduce reaction time and produce the desired product in high yield [1]. The development of heterogeneous catalytic systems for carrying out liquid-phase chemical and biochemical transformations is a major area of research, which has great significance for the development of cleaner and more efficient processes due to its easy catalyst separation, recovery, and recycling [2,3]. Chitosan, a natural biopolymer derived from polysaccharides, has garnered significant attention across scientific and engineering fields [4]. Chitosan-based catalysts hold promise for organic catalysis because of their “green” accessibility. While most research has focused on chemically modifying chitosan to create functional derivatives for specific purposes [5], its

advantages are manifold: cost-effectiveness, eco-friendliness, hydrophilicity, modifiability, chemical stability (with high thermal resistance up to 280 °C), non-toxicity, biodegradability, and metal-anchoring capabilities [6–11]. Its hydroxyl and amino groups, along with its insolubility in organic solvents, make it particularly appealing [12,13]. Macquarrie and Hardy reported a survey of methodology for the functionalization of chitosan and how the functional chitosans are used in catalysis [2]. Numerous documented studies have illustrated diverse uses of chitosan-based catalysts across chemical synthesis [2,3,14–16], with a particular focus on thiazole synthesis [17–20].

Ultrasound-assisted reactions provide the benefits of faster reaction times, a straightforward experimental strategy, excellent yields, improved selectivity, and clean procedures [17,21]. One of the numerous benefits of ultrasonic irradiation is its capacity to be crucial in chemistry, particularly in cases where traditional procedures need harsh temperatures or prolonged reaction periods [22–24]. The susceptibility of bacteria to antimicrobial medicines is a matter of great concern in both community and hospital settings [25–28]. Diseases caused by bacteria have had a significant global impact, resulting in high mortality rates. Therefore, the need for effective therapy has produced extensive research on novel antimicrobials [29–32]. In this context, the development of pharmaceutically active drugs has increasingly relied on the use of heterocyclic scaffolds, many of which contain nitrogen. This is evident from the abundance of active derivatives currently available [33–37]. It is important to note that the incorporation of hetero-atoms into these molecules is not arbitrary but is based on their physiochemical properties and, more importantly, on achieving ideal results for the absorption, distribution, metabolism, and excretion (ADME) of the main therapeutic agents [38,39]. The thiazole scaffold has received significant attention from numerous researchers due to its medicinal value, resulting in the synthesis and design of various compounds containing thiazoles with diverse pharmacological activities. The thiazole nucleus serves as an interesting building block in natural and synthetic compounds, exhibiting good antibacterial activity [40,41]. Similarly, thiophene, another heterocyclic molecule, has attracted the interest of medicinal and chemical biologists. Thiophene derivatives have demonstrated a range of biological properties, including antibacterial activity [42,43].

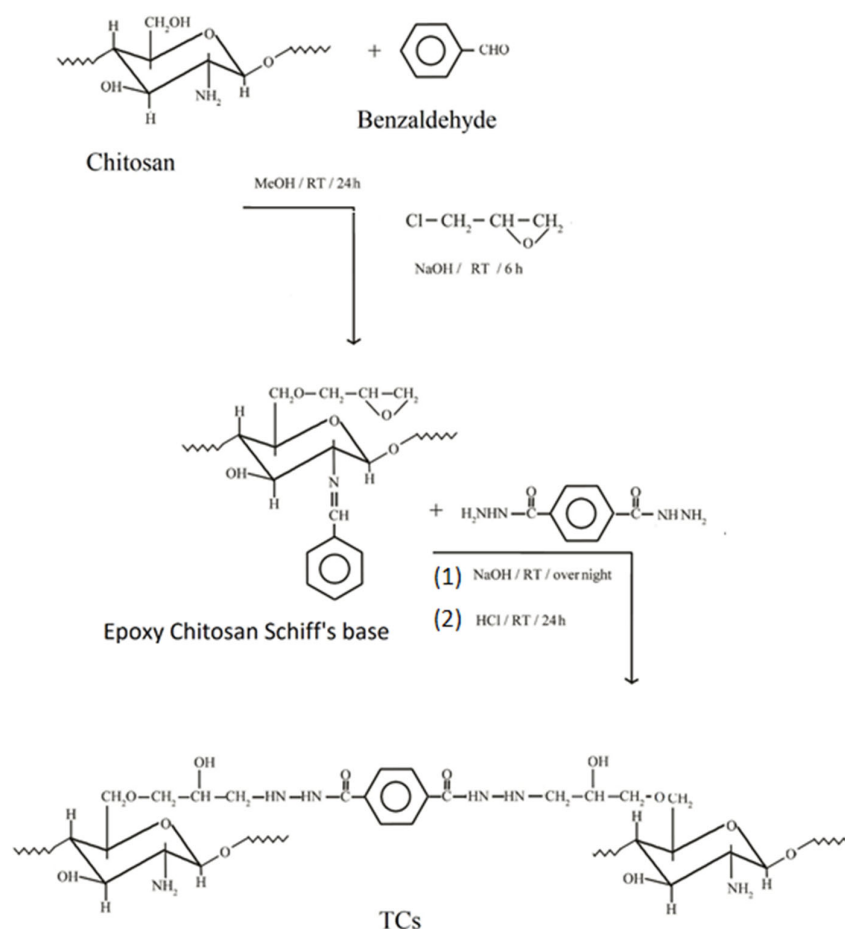
On the other hand, thiazole and thiadiazole derivatives constitute crucial frameworks in the realm of medicinal chemistry. An exploration of the literature highlights their significant role encompassing a diverse array of biological effects [44–48], notably including antimicrobial properties [49–53].

In light of these findings, molecular docking studies were conducted on substances that show high efficacy against the tyrosyl-tRNA synthetase in *Staphylococcus aureus* (PDB ID: 1JII). Antibiotics such as Norfloxacin are frequently used in the treatment of various bacterial diseases [54]. Furthermore, the structure–activity relationship (SAR) and druglikeness analysis of the reported derivatives were also investigated. Hence, in continuation of our efforts in green chemistry research [55–62] and considering the biological importance of the thiazole derivatives [46,63–68], the present work aimed to synthesize, characterize, and investigate the catalytic potency of the TCs in the construction of functionalized thiazole derivatives by simple, convenient, and ecofriendly synthetic methodology by using simple starting materials under ultrasonic irradiation.

## 2. Results and Discussion

In comparison to the parent chitosan, the TCs derivative contains a significantly higher number of function groups, which serve as active centers for the adsorption of reactant molecules and lead to the synthesis of intermediate compounds. The product is created by the breakdown of this intermediate molecule. As soon as the products are created, they are instantly desorbed from the catalyst's surface (Scheme 1).





**Scheme 1.** Preparation of TCs hydrogel.

## 2.1. Characterization of the TCs Hydrogel

### 2.1.1. Fourier Transform Infrared (FTIR) Analyses

The FTIR spectra of Cs and TCs are shown in Figure 1. As can be observed, the vibrations of the TCs differ significantly from those of the parent Cs. Characteristic bands for the saccharide moiety of the chitosan were observed at 1155, 1073, 1030, and 895  $\text{cm}^{-1}$ . The stretching vibration band attributed to  $-\text{NH}_2$ ,  $-\text{OH}$  groups, and their hydrogen bonds appeared in the range of 3200–3600  $\text{cm}^{-1}$  (strong and wide); its locations at 3460 and 3190  $\text{cm}^{-1}$  indicated the presence of the  $-\text{NH}_2$  groups. The peak at 2923  $\text{cm}^{-1}$  is attributed to the C–H bonds in the glucopyranose ring. Two vibration bands of a comparatively lower intensity appeared at 1653 and 1567  $\text{cm}^{-1}$ , corresponding to amide I and amide II, respectively. This demonstrated that Cs had significant deacetylation. The overlapping amide I and  $-\text{NH}_2$  bending vibrations cause the strong band at 1653  $\text{cm}^{-1}$  [12].

Chitosan Schiff's base displayed that the two peaks that related to the primary  $\text{NH}_2$  groups of chitosan at 3460 and 3190  $\text{cm}^{-1}$  have vanished entirely and only one broad peak has appeared at around 3439  $\text{cm}^{-1}$ , assigned to the hydrogen-bonded hydroxyl groups. This indicates the consuming of all the primary  $\text{NH}_2$  groups via their condensation reaction with the carbonyl groups of benzaldehyde molecules, affirming the protection of all the primary  $\text{NH}_2$  groups of chitosan. Furthermore, some new peaks have appeared at 692 and 757  $\text{cm}^{-1}$  related to an out-of-plane monosubstituted benzene ring and at 1579, 1555, and 1493  $\text{cm}^{-1}$ , corresponding to the benzene ring and C=N group, respectively [9].

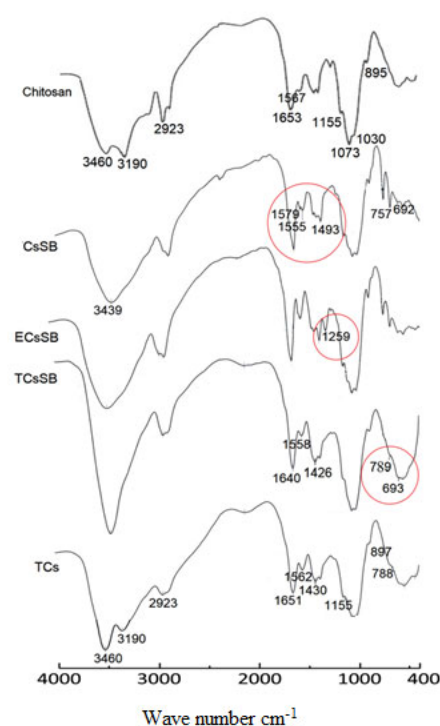


**Figure 1.** FTIR spectra of chitosan and TCs hydrogel.

The FTIR spectrum of epoxy chitosan Schiff's base exhibited an additional specific peak at  $1259\text{ cm}^{-1}$  related to  $\text{C-O-C}$  linkage of the epoxy ring [9]. TCsSB formation was confirmed by evanescence of the peak of the  $\text{C-O-C}$  linkage of the epoxy ring at  $1259\text{ cm}^{-1}$ , denoting the opening of all the epoxy rings through their crosslinking with terephthalohydrazide in chitosan. Moreover, the absorption peaks corresponding to the  $\text{-CO-}$ ,  $\text{-NH-NH-}$ , and terephthalohydrazide ring emerged at  $1640\text{ cm}^{-1}$  (indicating hydrazide CO),  $3432\text{ cm}^{-1}$  (denoting  $\text{-OH}$ ), as well as  $789$ ,  $692$ , and  $1558\text{ cm}^{-1}$  (representing di-substituted benzene rings). Despite the FTIR spectrum of TCs showing identical absorption bands to that gained in TCsSB, it was noticed that the doublet bands for the primary  $\text{NH}_2$  groups at  $3460$  and  $3190\text{ cm}^{-1}$  have reappeared. This indicates a deprotection of all the primary amine groups of chitosan chains in TCs.

### 2.1.2. X-ray Diffraction (XRD) Analyses

Figure 2 displays the XRD modality of Cs and TCs hydrogel. XRD mode for Cs showed two characteristic peaks at  $2\theta = 10^\circ$  and  $20^\circ$  that are attributed to chitosan amorphous and crystalline structure, respectively [8]. This is because, in addition to the core amino groups, there are several polar hydroxyl groups present, allowing for a significant amount of inter- and intramolecular H-bonding.

Chitosan's morphology was significantly altered by chemical cross-linking at OH groups on C6 caused by the incorporation of a terephthalohydrazido moiety. This may be attributable to the chains' separation from one another, which significantly decreased the crystalline component and significantly increased the amorphous component. As evidenced by the XRD pattern of TCs, the peak at  $2\theta = 10^\circ$  has totally vanished and the intensity of the peak at  $2\theta = 20^\circ$  has significantly diminished (Figure 2). The large voids that resulted from the removal of the benzaldehyde moieties led to the generation of a structure that is considerably more open and approachable.

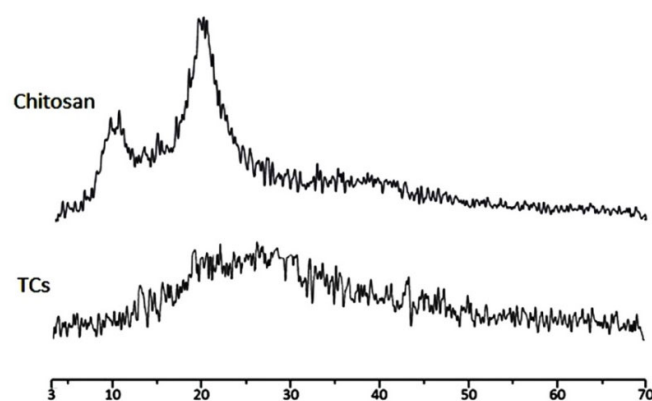


**Figure 2.** XRD patterns of chitosan and TCs hydrogel. Diffraction angle:  $2\theta$  (degrees).

### 2.1.3. Scanning Electron Microscopy (SEM) Analyses

Chitosan and TCs' surface morphologies were observed using SEM, and their SEM images are displayed in Figure 3. The morphological structure of chitosan exhibited significant changes after cross-linking with terephthalohydrazido linkages. It turned from a highly smooth surface to a highly rough surface full of pores. It seems that crosslinking apart the chains from each other and destroying many of the hydrogen bonds between the chitosan chains leads to an amorphous, open, and porous structure.

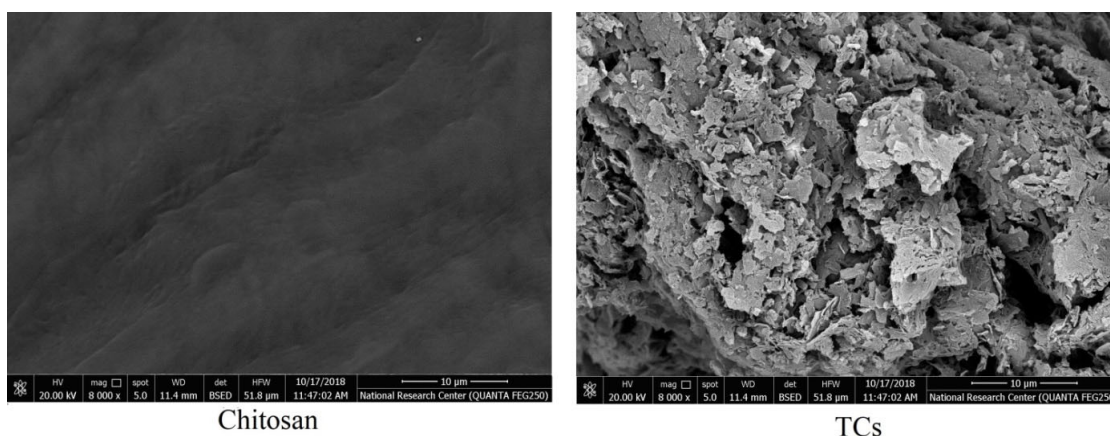


**Figure 3.** SEM images of chitosan and TCs hydrogel.

### 2.1.4. Thermogravimetric (TG) Analyses

The good performance of the eco-friendly chitosan polymer as green catalyst requires boosting of its stability against thermal deterioration. One of the most efficacious operations to reinforce its thermal resistance is chemical crosslinking. So, chitosan is chemically modified, in this work, by incorporating terephthalohydrazido linkages between its chains to produce TCs hydrogel. For evaluation of the changes occurring in the chitosan thermal stability after the chemical crosslinking process, thermogravimetric analysis (TG) measurements are employed. The degradation manner and the thermal stability of the studied TCs hydrogel were investigated using a range of temperatures between 25 and 500 °C under a stream of nitrogen of 30 mL min<sup>−1</sup> and a heating rate of 10 °C min<sup>−1</sup>. The mass loss in both the TCs hydrogel and the parent chitosan, which were observed by TG measurements, were presented in Figure 4 and Table 1. The degradation pattern of TCs hydrogel was similar to that of the parent chitosan, comprising two special steps through which appreciable mass losses were observed. Initially, at a temperature range from 25 to 150 °C, the outcome of the first loss in mass for TCs was 5.88%, corresponding to 9% in the case of the virgin chitosan as listed in Table 1. This is related to vaporizing of the adsorbed water onto the investigated samples. In general, the mass loss that occurred above 100 °C is owing to

deterioration of the hydrogen bonds that link the molecules of water with the polar groups of the studied samples.

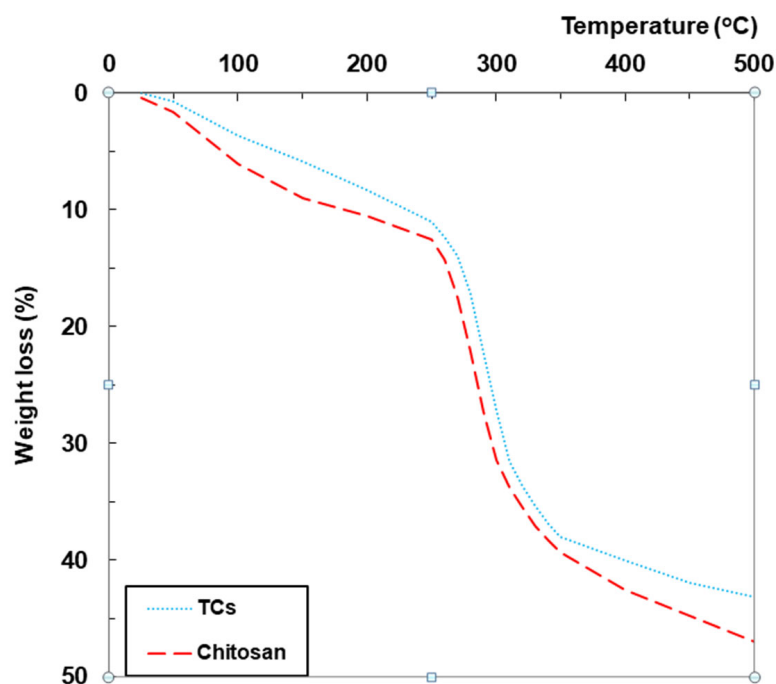


**Figure 4.** TG analysis of TCs hydrogel and chitosan measured under  $30 \text{ mL min}^{-1}$  nitrogen flow rate and at  $10^\circ \text{C min}^{-1}$  heating rate.

**Table 1.** TG measurements data of TCs hydrogel measured under  $30 \text{ mL min}^{-1}$  nitrogen flow rate and at  $10^\circ \text{C min}^{-1}$  heating rate.

Samples	1st Step					2nd Step			
	T(°C) at 5% Mass Loss	T(°C) at 10% Mass Loss	Tstart-Tend (°C)	Mass Loss%	Tpeak (°C)	Tstart-Tend (°C)	Mass Loss%	Tpeak (°C)	Residue%
Chitosan	90.32	185.26	25–150	9.00	57.14	250–500	34.53	300.56	52.94
TCs	130.45	235.37	25–150	5.88	59.61	250–500	32.22	482.43	56.78

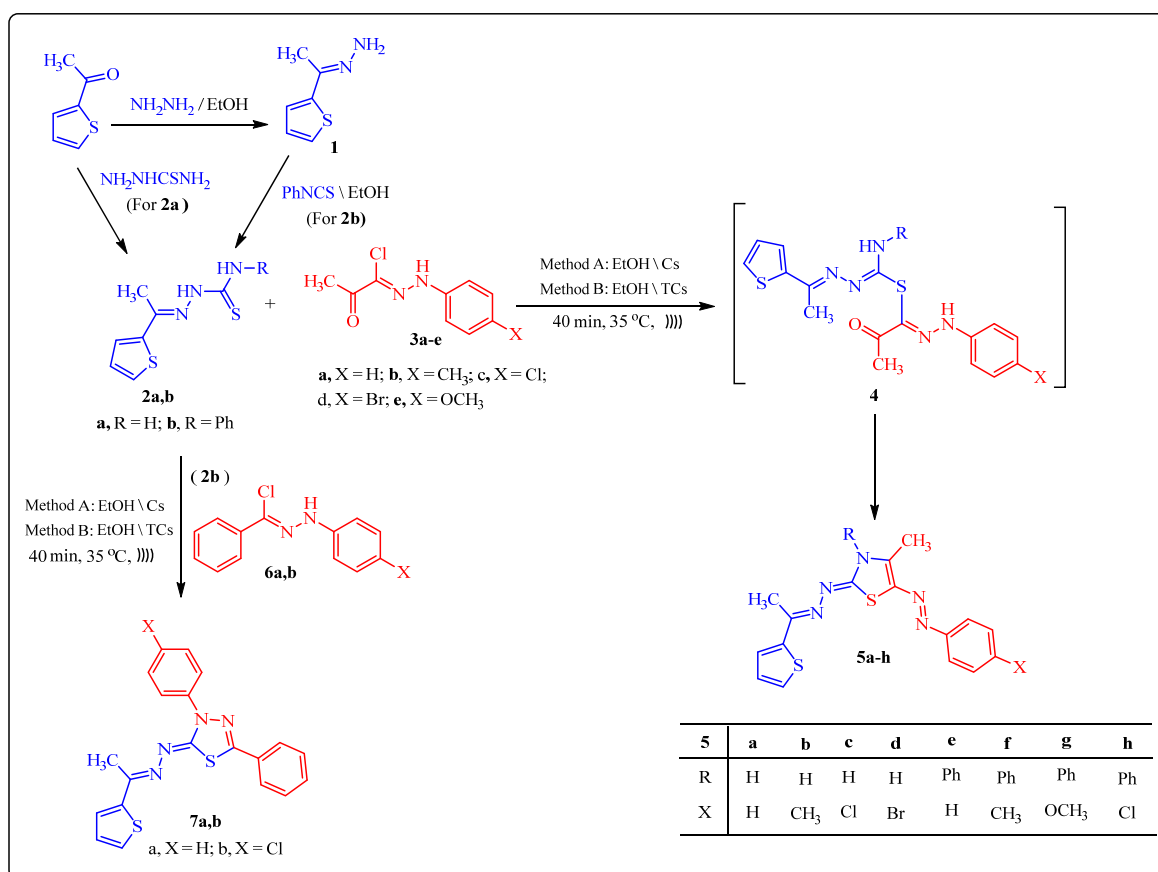
Secondly, a sharp thermal degradation process was observed that commenced near to  $250^\circ \text{C}$ . TCs has a residue of 56.78% of its weight, at  $500^\circ \text{C}$ , versus 52.94% of the parent chitosan, as listed in Table 1. This indicated that TCs and chitosan have been decomposed via some complicated reactions, encompassing both the dehydration and random scission of their saccharide moieties and also liberating and vaporizing the small molecules produced from decomposition.

Further, the mass loss in TCs may be ascribed to cyclodehydration reaction by losing water from the hydrazide linkages into 1,3,4-oxadiazole nuclei. This reaction is not a truly decomposing process, but it is a thermo-chemical transforming operation into heterocyclic polymers rich with high thermally stable 1,3,4-oxadiazole rings [69,70]. It is notable that TCs is more thermally stable than chitosan, as judged by its higher residual weight together with its lower mass loss at any of the examined temperatures. This is due to crosslinking of chitosan chains by terephthalohydrazido possessing both aromatic rings and hydrazide groups that have high resistance toward the elevated temperatures.

## 2.2. Synthesis of Thiazole and Thiadiazole Derivatives Using TCs as Basic Heterogeneous Catalyst

In this article, we would like to provide a simple and effective method for producing some new thiazoles and thiadiazoles. The active key N-phenyl-2-(1-(thiophen-2-yl) ethylidene)hydrazine-1-carbothioamide **2b** was initially created by condensing (1-

(thiophen-2-yl)ethylidene)hydrazine **1** [71] with phenylisothiocyanate in refluxing EtOH solution (Scheme 2). By reacting equimolar amounts of thiosemicarbazone derivative **2a** [72] or **2b** with 2-oxo-N-arylpropanehydrazonoyl chlorides **3a–e** [73] in the presence of Cs and TCs under ultrasonic irradiation, new thiazole derivatives **5a–h** were produced (Scheme 2). Based on spectrum IR, MS,  $^1\text{H-NMR}$ , and elemental analyses, the chemical structure of all newly produced thiazoles **5a–h** was confirmed. The  $^1\text{H-NMR}$  of isolated derivatives **5a–h**, which showed the anticipated signals for the proposed structure, validated their structures (see Section 2.1 Experimental section). The electronic absorption spectral data of compounds **5e–h** in DMSO exhibited two characteristic absorption bands at  $\sim 370$  and  $260$  nm, which are similar to that of the typical hydrazone chromophore [74].

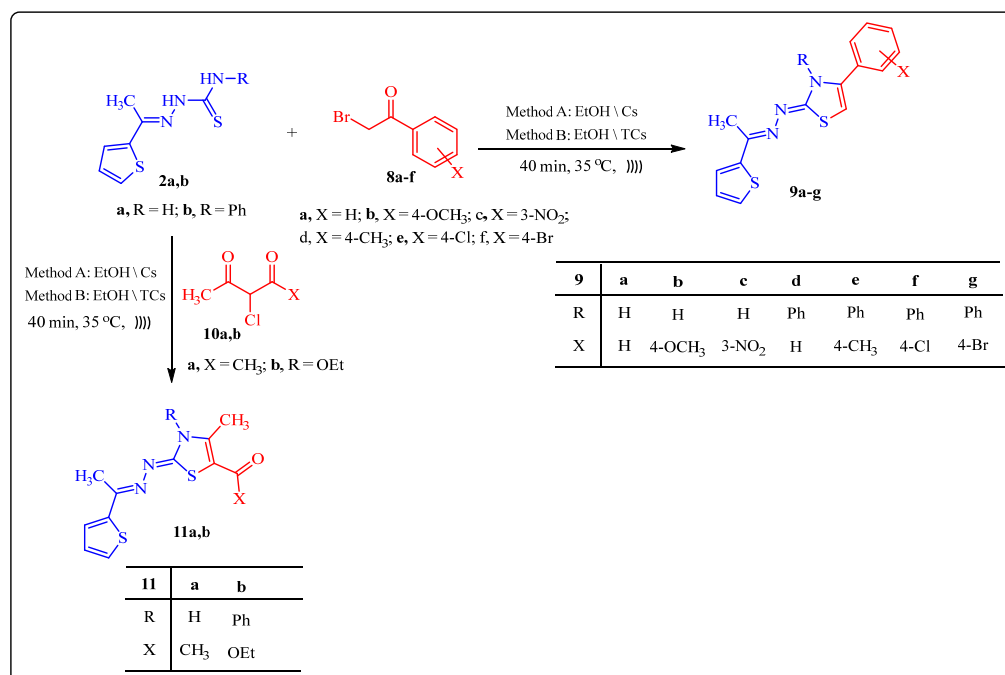


**Scheme 2.** Synthesis of thiazoles **5a–h** and thiadiazoles **7a,b**.

Also, N-arylbenzohydrazonoyl chlorides **6a,b** [75] reacted with the compound **2a** and **2b** to furnish the corresponding 1,3,4-thiadiazole derivatives **7a,b** (Scheme 2). Through analytical and spectral data analysis, the structure of products **7a** and **7b** was also established (see Section 2.1).

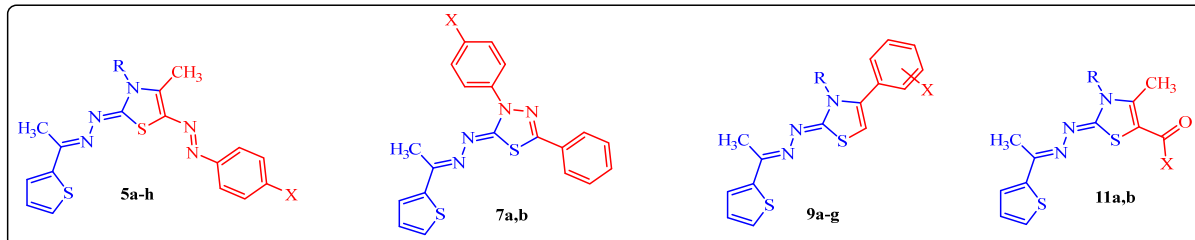
Our study was extended to study the effect of treating compounds **2a** and **2b** with 2-bromo-1-arylethan-1-ones **8a–f** under the same reaction conditions, as stated in Scheme 3, yielding the corresponding thiazoles **9a–g** as the final products utilizing Cs and TCs as basic catalysts. The yield percentage of the obtained products **9a–g** was then investigated (Table 2). The chemical structure of the target compounds **9a–g** was established based on IR,  $^1\text{H-NMR}$ ,  $^{13}\text{C-NMR}$ , and MS spectra (see Section 2.1).





**Scheme 3.** Synthesis of thiazoles **9a–g** and **11a,b**.

**Table 2.** The yield% of thiazoles **5a–h**, **10a–g**, and **12a,b** and thiadiazoles **8a,b** utilizing Cs and TCs under ultrasonic irradiation at 35 °C for 40 min.



Compd. No.	R	X	(%) YieldUsing Cs	(%) YieldUsing TCs	M.p.(°C) <sup>a</sup>	Reference
5a	H	H	77	88	186–188	[72]
5b	H	Me	76	86	172–174	[72]
5c	H	Cl	79	87	216–218	[72]
5d	H	Br	75	88	203–205	[72]
5e	Ph	H	80	87	216–218	-
5f	Ph	Me	81	86	207–209	-
5g	Ph	OMe	78	85	173–175	-
5h	Ph	Cl	80	88	238–240	-
7a	-	H	69	80	160–162	-
7b	-	Cl	72	84	183–185	-
9a	H	H	82	89	261–263	[76]
9b	H	MeO	78	88	250–252	[77]
9c	H	NO <sub>2</sub>	80	87	246–248	[76]
9d	Ph	H	82	91	212–214	-
9e	Ph	Me	84	90	201–203	-
9f	Ph	Cl	83	92	229–231	-
9g	Ph	Br	82	93	215–217	-
11a	H	Me	77	87	220–222	[76]
11b	Ph	OEt	79	90	231–233	-

<sup>a</sup> M.p.: melting point; solvent of crystallization: EtOH or DMF.

Finally, in a similar manner, when compounds **2a** and **2b** were allowed to react with  $\alpha$ -chloro compounds **10a,b**, thiazoles **11a,b** were obtained in good yields as outlined in Scheme 3. The yield percentage of the obtained products **9a–g** was then investigated (Table 2). The structure of the isolated product **11** was inferred from its IR and  $^1\text{H-NMR}$  spectral data and elemental analysis (see Section 2.1).

Initial studies were conducted to find the optimum basic catalyst (Table 2).

As shown in Table 2, under ultrasonic irradiation, TCs performed better as a basic catalyst than Cs. Under the same reaction conditions, Cs is switched out for TCs, increasing the yields of the desired products **5a–h**, **7a,b**, **9a–g**, and **11a–b**.

The ideal experimental parameters (including catalyst loading, solvent, reaction time, and temperature) for the reaction of **2a** + **3a** with a catalytic amount of TCs under USI to produce the thiazole derivative **5a** are as follows:

- The amount of the catalyst used for synthesis of compound **5a** was examined as shown in Table 3, entries 1–4. With a catalyst concentration of 10 mol%, the highest results (88%) were attained (Table 3, entry 2).
- The effectiveness of the different solvents was then examined using USI (Table 3, entries 3, 5, 6). According to a screening of several solvents, EtOH produced product **5a** with the greatest yield and the quickest reaction rate (Table 3, entry 3).
- The reaction time was assessed using USI (Table 3, entries 3, 7–9). Product **5a** was best formed in 40 min (Table 3, entry 3).
- The effect of temperature on the reaction was examined; the outcomes are shown in Table 3 (entries 3, 10–13). As indicated in Table 3, employing USI led to a sequential elevation of reaction temperatures from 25 °C to 30 °C, 35 °C, and 40 °C. This caused a corresponding escalation in product yields, with enhancements of 77%, 83%, and 88%, respectively. The optimal temperature was finally determined to be 35 °C (Table 3, entry 3).

**Table 3.** Reaction conditions optimization for synthesis of thiazole **5a** (catalyst loading, solvent, reaction time, and temperature).

Entry	TCs (mol%)	Solvent	Time (min)	Temperature (°C)	Yield (%)
1	2	EtOH	40	35	79
2	5	EtOH	40	35	83
3 <sup>a</sup>	10	EtOH	40	35	88
4	20	EtOH	40	35	88
5	10	DMSO	40	35	81
6	10	Dioxane	40	35	85
7	10	EtOH	20	35	81
8	10	EtOH	30	35	85
9	10	EtOH	50	35	88
10	10	EtOH	40	25	77
11	10	EtOH	40	30	83
12	10	EtOH	40	35	88
13	10	EtOH	40	40	88

<sup>a</sup> The best reaction condition for the synthesis of component **5a**.

Additionally, the possibility of the TCs to be recycled as a fundamental catalyst was investigated. To reuse the catalyst, it should be washed with distilled water and dried at 60 °C for 30 min. The catalyst might be utilized three times under optimal conditions without suffering a substantial loss in catalytic efficacy (Table 3). Reusability of the TCs as a catalyst was tested four times and its efficiency to produce the target product **5a** decreased from 88% to 51% at ideal conditions (10 wt%, 35 °C, and 40 min) (Table 4). The results of recycling experiments in Table 4 showed that, without noticeably reducing the product yield, the recovered catalyst can be utilized in future reactions at least three more times.

**Table 4.** Recyclability of TCs as basic catalyst.

State of Catalyst	New Catalyst	Recycled Catalyst				
		(1)	(2)	(3)	(4)	(5)
Product <b>5a</b> (% Yield)	88	85	82	79	51	27

According to Table 3, the ideal conditions for synthesizing product **5a** are a reaction between **2a** + **3a** in ethanol under ultrasonic irradiation in the presence of TCs (10% wt) at 35 °C for 40 min. Thus, irradiation of thiosemicarbazone derivatives **2a** and **2b** with the other hydrazonoyl chlorides **3b–e** and **6a,b** or 2-bromo-1-arylethan-1-ones **8a–f** or  $\alpha$ -chloroketones **10a,b** under ideal conditions produced the products **5b–h**, **7a,b**, **9a–g**, and **11a,b**, respectively (Schemes 2 and 3).

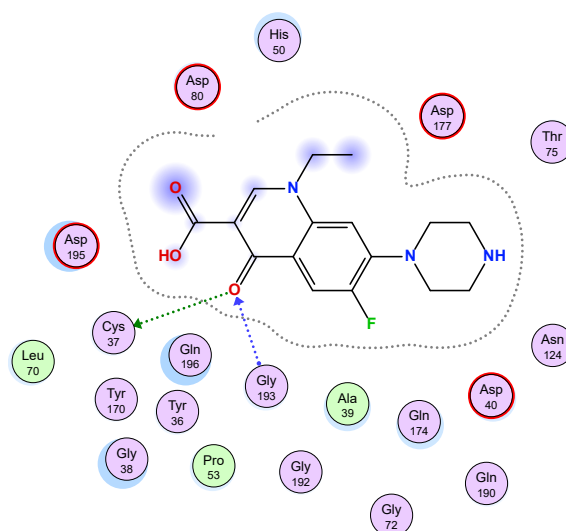
Thus, TCs was utilized as an environmentally friendly heterogeneous basic catalyst for the effective synthesis of biologically active thiazole derivatives, exhibiting superior performance over Cs. The catalyst demonstrated successful reusability up to three cycles at a 10 wt% loading, retaining its catalytic efficacy. This strategy highlights its ecological benefits alongside advantageous features, such as gentle reaction conditions, swift reaction kinetics, notable yields, and reusability. The potential of TCs as an eco-friendly biopolymer-based catalyst opens avenues for further exploration in heterogeneous synthesis of various heterocyclic compounds.

### 2.3. Molecular Docking Studies

Molecular docking studies define the interactions between the designed compounds with the targeted protein. Docked molecules were graded on the basis of the binding affinity scores and presence of prominent hydrogen bonds, arene interaction, and RMSD (Table 5). The overall docking results were compared to norfloxacin. Norfloxacin demonstrated the interactions with the residues of protein (Figure 5). According to the simulation of molecular docking results, the test ligands used in this research are known to have higher binding energies than standard inhibitor (−7.10 kcal/mol). The most potent compounds exhibit binding energy values between −6.21 and −7.85 kcal/mol docked against PDB 1JJJ. As shown in Table 5, for the test compound **5g**, sulfur atom interacted as two *H*-bond donors with the Asp40 and Thr75. In addition, the thiazole ring formed *pi-H* bond interaction with Asp40. The 3D model of compounds **7b** and **9a** showed one hydrogen bond donor between its sulfur of thiophene ring with Gly49. Additionally, in compound **10a**, another hydrogen bond donor between its sulfur of thiazole ring and the side chain Val191 formed, as well as in compound **9b**, with three hydrogen bond donors, two with Cys37 and the third one with Val191. In addition, the thiazole ring formed a *H-pi* bond interaction with Tyr36. As shown, compound **9d** formed one *H*-bond donor between its sulfur of thiazole moiety with Val191. The 3D model of compounds **9f** and **9g** showed one hydrogen bond donor between chloro and bromo atoms with Asp177, respectively, as well as in compound **11a** with two hydrogen bonds, one donor between an atom of nitrogen in the thiazole moiety with Asp80 and another acceptor between an oxygen atom with a side chain through Lys84. Finally, the 3D model of the **11b** showed one hydrogen bond donor between its sulfur of thiophene ring with Cys37 (Table 6).

**Table 5.** Docking score (kcal/mol), no. of *H*-bonding, no. of arene interaction, and RMSD kcal·mol<sup>−1</sup>Å<sup>−1</sup> formed between most synthesized compounds with 1JJJ receptors.

Compd. No.	Docking Score (kcal/mol)	No. of Hydrogen Bonding	No. of Arene Interaction	RMSD kcal·mol <sup>−1</sup> Å <sup>−1</sup>
5e	−7.36	-	-	0.84
5f	−7.49	-	-	1.08
5g	−7.78	1 (Asp40) 1 (Thr175)	1 (pi- <i>H</i> ) [Asp40]	1.08
5h	−7.85	-	-	1.43
7a	−7.26	-	1 (pi- <i>H</i> ) [His50] 1 (pi- <i>H</i> ) [Asp80]	1.00
7b	−7.60	1 (Gly49)	-	1.03
9a	−6.48	1 (Cly49) 1 (Vall91)	-	1.54
9b	−7.15	2 (Cys37) 1 (Vall91)	1 ( <i>H</i> -pi) [Tyr36]	1.73
9c	−6.76	-	-	0.80
9d	−7.23	1 (Vall91)	-	2.24
9e	−7.25	-	-	2.06
9f	−7.3	1 (Asp177)	-	0.87
9g	−7.44	1 (Asp177)	-	0.83
11a	−6.21	1 (Asp80) 1 (Lys84)	-	1.25
11b	−7.13	1 (Cys37)	-	1.09
Norfloxacin	−7.10	1 (Cys37) 1 (Gly193)	-	0.83

**Figure 5.** 2D model of norfloxacin (a reference ligand) with 1JJJ.

**Table 6.** D and 2D ligand interactions within the binding site of 1JJ for most compounds.

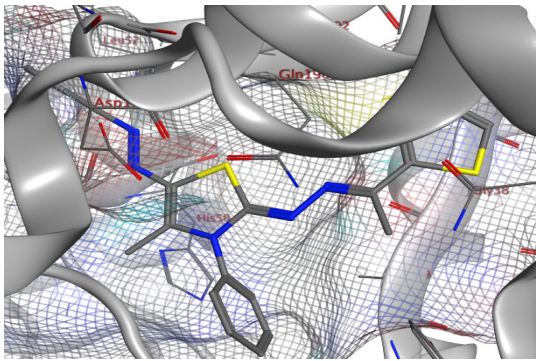
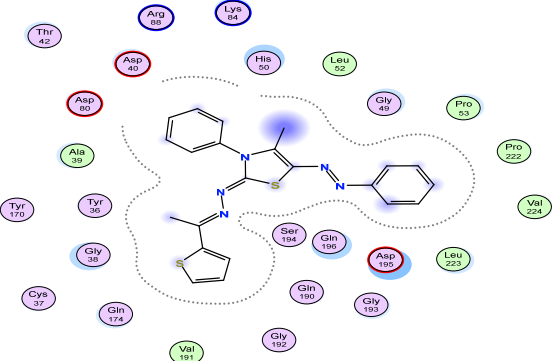
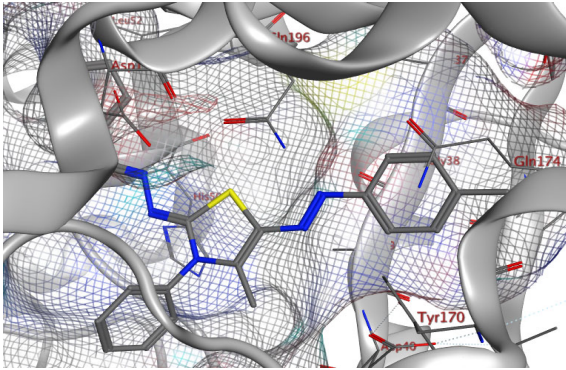
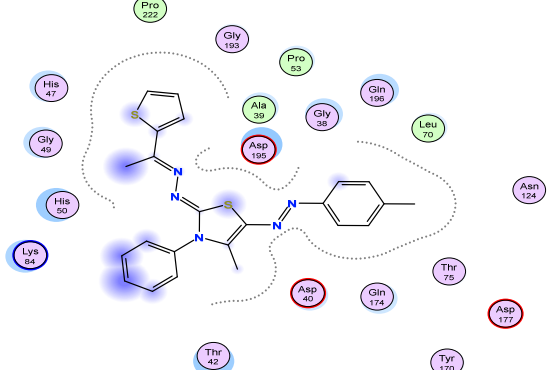
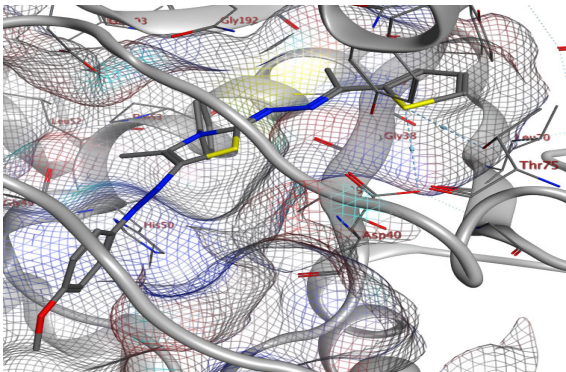
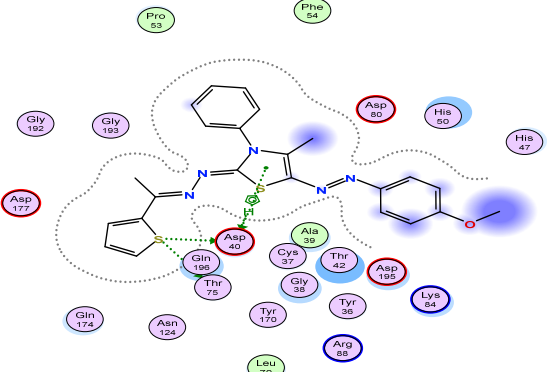
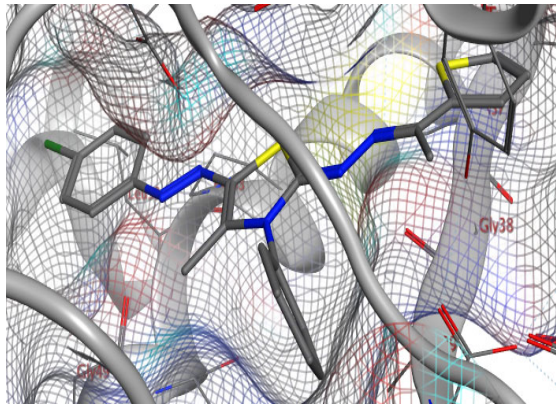
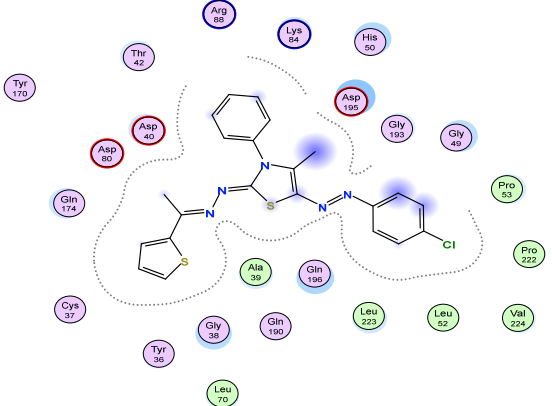
Compd. No.	3D Ligand Interaction	2D Ligand Interaction
5e		
5f		
5g		
5h		



Table 6. Cont.

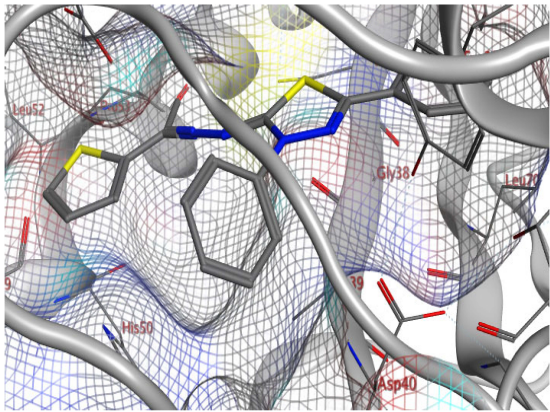
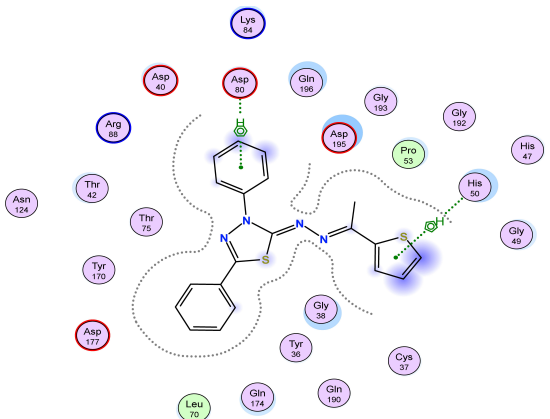
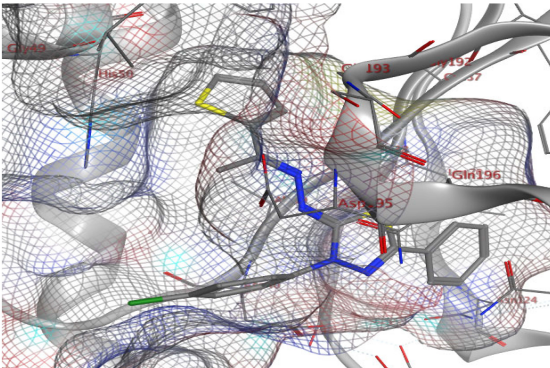
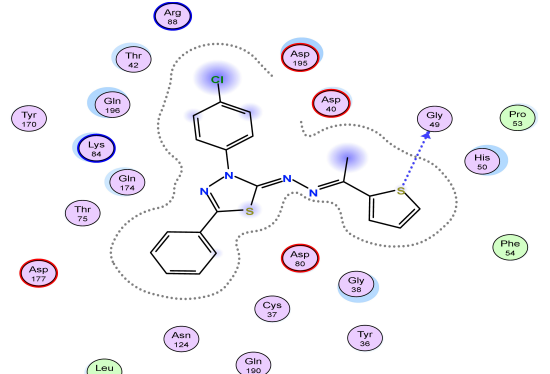
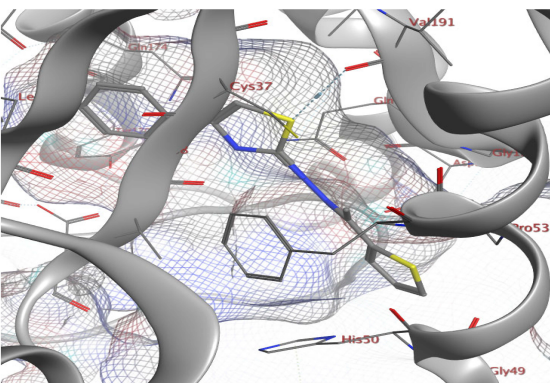
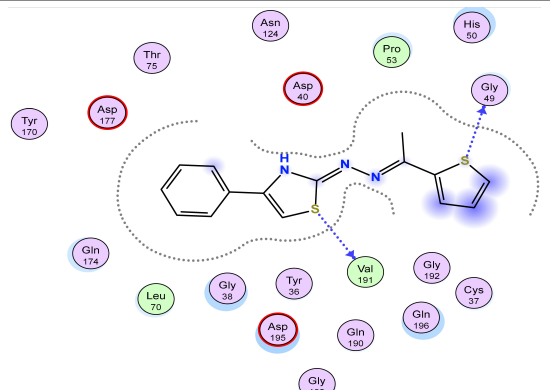
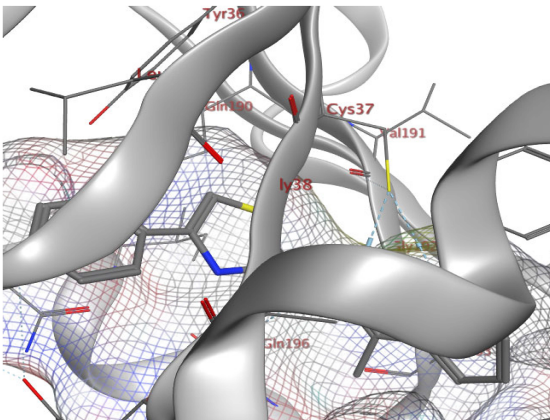
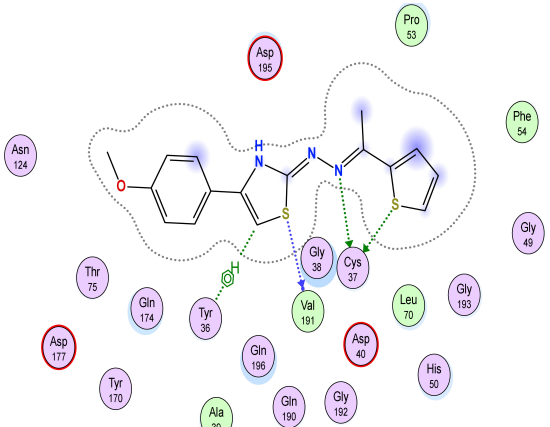
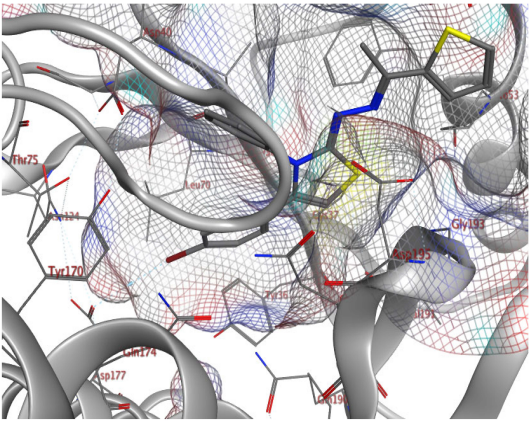
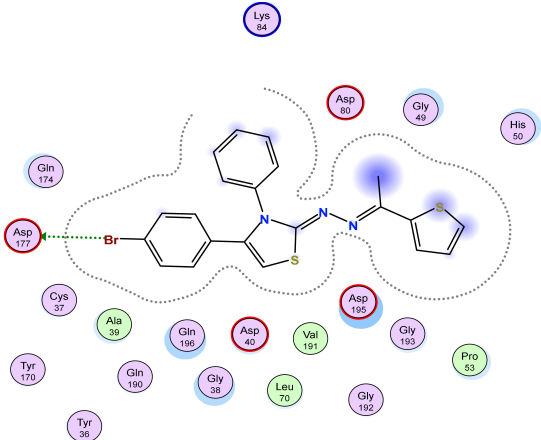
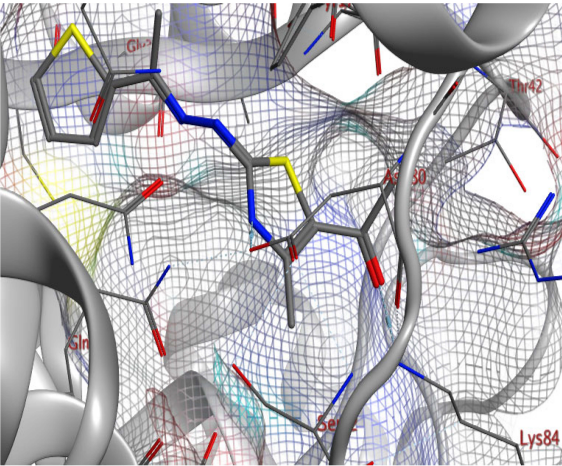
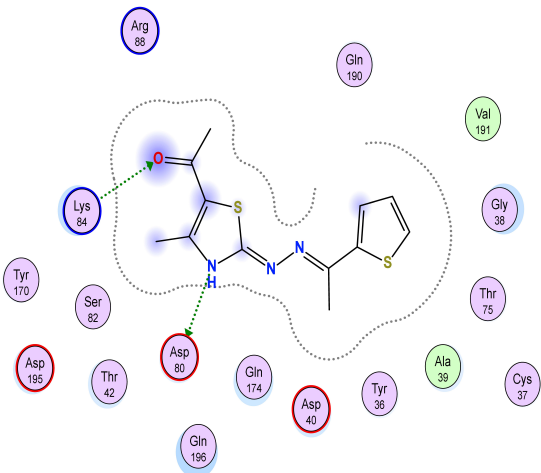
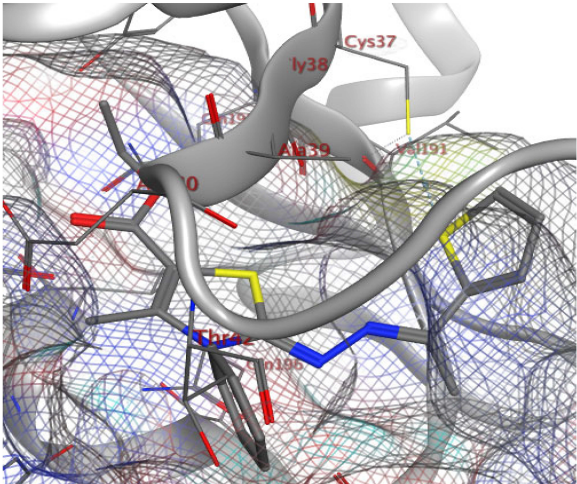
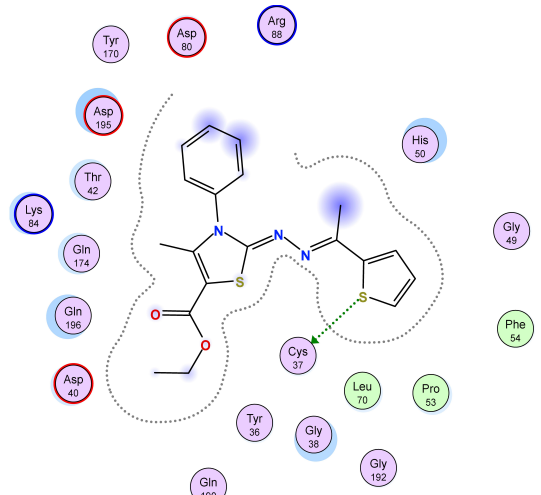
Compd. No.	3D Ligand Interaction	2D Ligand Interaction
7a		
7b		
9a		
9b		

Table 6. Cont.

Compd. No.	3D Ligand Interaction	2D Ligand Interaction
9c		
9d		
9e		
9f		



Table 6. Cont.

Compd. No.	3D Ligand Interaction	2D Ligand Interaction
9g		
11a		
11b		

### SAR Analysis for Synthesized Thiazole Derivatives

Notably, by employing extension and derivatization techniques on thiazole derivatives, we observed that compounds, particularly those with electron-withdrawing groups, exhibited significant activity [78,79]. Among all the thiazole derivatives, compounds carrying a para group on the phenyl moiety displayed the highest antimicrobial activities [78]. Researchers synthesized and examined various substitutions over the thiazole ring, with

4-ClC<sub>6</sub>H<sub>4</sub>, 4-OCH<sub>3</sub>C<sub>6</sub>H<sub>4</sub>, and 4-CH<sub>3</sub>C<sub>6</sub>H<sub>4</sub> being the preferred substitutions that had a significant impact on the compound's activity [80,81]. In terms of cytotoxicity, compounds with electron-donating substituents in the para position of the benzene ring demonstrated the following trend: OCH<sub>3</sub> > CH<sub>3</sub> [82]. Conversely, the absence of substitution on the phenyl ring resulted in the most noticeable decrease in activity within the series [83].

*2.4. ADMET Property Studies: The Absorption, Distribution, Metabolism, and Excretion (ADME) Aspects of the Medications Were Calculated Using the SwissADME, Which Predicts Physically and Pharmaceutically Significant Components of Organic Compounds [84]*

#### In Silico ADMET Study

SwissADME, an online tool, is a dependable resource that allows users to assess the chemical similarity of a substance to a medication and understand its behavior within the body. To evaluate the physicochemical descriptors of the most active derivatives (**5h**, **7b**, **9b**, **9g**, and **11b**) in comparison to norfloxacin, a reference drug, computational analysis was conducted using the web resource SwissADME (<http://swissadme.ch/index.php>, accessed on 5 July 2023) as previously described [85]. The evaluation focused on essential physicochemical characteristics, including molecular weight, lipophilicity, the number of cases of HBDs and HBAs (hydrogen bond donors and acceptors), rotatable bonds (ROT), and polar surface area (PSA). Table 7 presents the predicted descriptors, categorized as molecular properties, pharmacokinetics, druglikeness, and medicinal chemistry. Drug-like compounds that have undergone considerable research provide interesting candidates for future therapeutic development. Derivatives **5h**, **7b**, and **9g** adhere to Lipinski's rule with one violation (MLOGP > 4.15), while all the most potent derivatives comply with the Veber rule without any violations.

**Table 7.** Prediction of molecular properties, pharmacokinetics, druglikeness, and medicinal chemistry of the most active derivatives, **5h**, **8b**, **10b**, **10g**, and **12b**, compared with norfloxacin.

Test Items	5h	7b	9b	9g	11b	Norfloxacin
<b>Molecular properties</b>						
PSA (°A <sup>2</sup> )	110.85	99.02	106.22	86.13	112.43	74.57
M. Wt.	451.99	410.94	329.44	454.41	385.50	319.33
HBA	4	3	3	2	4	5
HBD	0	0	1	0	0	2
NRB	5	4	4	4	6	3
<b>Pharmacokinetics</b>						
GI absorption	Low	High	High	Low	High	High
BBB permeant	No	No	No	No	No	No
P-gp substrate	No	No	No	No	No	Yes
Skin permeation (Log Kp) cm/s	−3.99	−4.21	−5.46	−4.47	−5.14	−8.98
<b>Drug likeness and Medicinal Chemistry</b>						
PAINS	1	0	0	0	0	0
Synthetic accessibility	4.06	3.73	3.23	3.61	3.79	2.46
Bioavailability Score	0.55	0.55	0.55	0.55	0.55	0.55
Lipinski Rule (violation)	Yes (1)	Yes (1)	Yes (0)	Yes (1)	Yes (0)	Yes (0)
Veber Rule (violation)	Yes	Yes	Yes	Yes	Yes	Yes

Regarding pharmacokinetic prediction, compounds **5h** and **9g** demonstrate low gastrointestinal tract permeability, while the others exhibit high permeability. All the most potent derivatives are non-substrates for P-glycoprotein (P-gp). A compound classified as a P-gp substrate reduces drug accumulation in multidrug-resistant cells and is often associated with the development of drug resistance. In contrast, norfloxacin displays high gastrointestinal tract permeability and is a P-gp substrate. None of the compounds, including norfloxacin, are able to pass the blood–brain barrier (BBB). Additionally, the studied derivatives possess a permeability coefficient (LogKp) ranging from  $-5.46$  to  $-3.99$  cm/s, suggesting a limited ability to permeate the skin. In comparison, norfloxacin exhibits a predicted LogKp of  $-8.98$  cm/s, indicating a low chance of skin penetration.

Additionally, except for **5h**, none of the most potent derivatives and norfloxacin contain alarmed pan assay interference compounds (PAINs) in their structure. Furthermore, the majority of the most potent derivatives exhibit moderate synthetic accessibility with a score of 3.23 to 4.06, while norfloxacin demonstrates easy synthetic accessibility with a score of 2.46. The desired bioavailability score (ABS) for an effective oral medication was determined to be 0.55 for all ligands in this investigation, indicating that both tested compounds possess this value.

### 3. Materials and Methods

#### 3.1. Chemicals and Methods

All the chemicals and reagents used were of analytical quality and were purchased from Funakoshi Co. LTD (Tokyo, Japan), Alfa Aesar (Heysham, UK), and Sigma-Aldrich (Hamburg, Germany). Details of chemicals and reagents were inserted in Supplementary Information File.

Terephthalohydrazido cross-linked chitosan hydrogel (TCs), used as a catalyst in this work, was synthesized using a multistep reaction; first step includes protection of the chitosan amino groups via condensation with benzaldehyde molecules, forming chitosan Schiff base. The latter undergoes a further reaction with epichlorohydrin to produce epoxy chitosan Schiff base (second step), which can react easily with terephthaloyl dihydrazide to obtain terephthalohydrazido chitosan Schiff's base hydrogel (third step). The acid treatment of the latter generates terephthalohydrazido chitosan hydrogel (TCs) (Scheme 1). The preparation method's details were revealed in our previous study [8].

#### 3.2. Measurements

The used instruments are Shimadzu FTIR 8101 PC (Shimadzu Co., Mumbai, India) and Tescan Shimadzu FTIR (VSI Electronics Private Limited, Mohail, India); Shimadzu GCMS-QP1000 EX (Shimadzu Co., Kyoto, Japan). The  $^1\text{H}$ -NMR and  $^{13}\text{C}$ -NMR spectra were recorded using a Jeol-500 spectrometer (JEOL Canada, Inc.3275, Saint-Hubert, Canada) (500 MHz for  $^1\text{H}$ -NMR and 125 MHz for  $^{13}\text{C}$ -NMR); Electrothermal IA 9000 series, X-ray diffractometer (Bruker's D-8) (Malvern Panalytical Ltd. company, Liaoning, China); and Quanta scanning electron microscope (model FEG 250) (Technical Cell, Kolkata, India). Details of apparatus and instrumentations were inserted in Supplementary Information File.

#### 3.3. Synthesis of Thiosemicarbazone Derivative **2b** and Thiazole Derivatives **5a–h**, **9a–g**, **11a,b** and Thiadiazoles **7a,b**

##### 3.3.1. Synthesis of N-Phenyl-2-(1-(thiophen-2-yl)ethylidene)hydrazine-1-carbothioamide (**2b**)

A mixture of phenyl isothiocyanate (1.35 g, 10 mmol) and 1-(thiophen-2-yl) ethylidenehydrazine **1** [71] (1.40 g, 10 mmol) in methanol (30 mL) was refluxed for 4 h. The precipitated product was filtered off, and finally recrystallized from ethanol to give compound **2b**, as yellowish white crystals; 75% yield; mp  $191\text{--}193$  °C; IR (KBr):  $\nu$  3351, 3260 (2NH), 1601 (C=N)  $\text{cm}^{-1}$ ;  $^1\text{H}$ -NMR (DMSO- $d_6$ ):  $\delta$  2.38 (s, 3H, CH<sub>3</sub>), 7.07–7.61 (m, 8H, Ar-H), 9.68 (s, br, 1H, NH), 10.73 (s, br, 1H, NH) ppm;  $^{13}\text{C}$ -NMR (125 MHz, DMSO- $d_6$ )  $\delta$ : 15.7 (CH<sub>3</sub>), 114.7, 125.0, 126.2, 128.3, 128.7, 128.9, 139.4, 143.1, 146.3, (Ar-C and C=N),



176.8 (C=S) ppm; MS  $m/z$  (%): 275 ( $M^+$ , 73). Anal Calcd for  $C_{13}H_{13}N_3S_2$  (275.06): C, 56.70; H, 4.76; N, 15.26. Found: C, 56.53; H, 4.71; N, 15.14%.

### 3.3.2. General Procedure for Synthesis of Thiazoles **5a–h**, **9a–g**, **11a,b** and Thiadiazoles **7a,b**

#### Method A

Chitosan (15 mol%) was added to a mixture of 2-(1-(thiophen-2-yl)ethylidene)hydrazine-1-carbothioamide **2a** [72] or *N*-phenyl-2-(1-(thiophen-2-yl)ethylidene)hydrazine-1-carbothioamide **2b** (1 mmol) and appropriate hydrazonoyl halides **3a–e** [73] or **6a,b** [75] or 2-bromo-1-arylethan-1-ones **8a–f** or  $\alpha$ -chloroketones **10a,b** (1 mmol) and these substances were exposed to ultrasonic irradiation for 40 min at 35 °C. To obtain derivatives of the corresponding compounds **5a–h**, **7a,b**, **9a–g**, and **11a,b**, the chitosan was removed via filtration from the hot solution, followed by further filtering of the precipitated product that had formed and finally crystallization from EtOH or DMF.

#### Method B

Employing terephthalohydrazido-chitosan hydrogel (TCs) (10 mol%) instead of chitosan in the same manner as method A, the physical constants and analytical information for the new synthesized products **5e–h**, **7a,b**, **9d–g**, and **11b** are listed below, while details of the physical constants and analytical information for the known products **5a–d**, **9a–c**, and **11a** were inserted in Supplementary Information file.

4-Methyl-5-(phenyldiazenyl)-2-(2-(1-(thiophen-2-yl)ethylidene)hydrazinyl)thiazole (**5a**) [72].

4-Methyl-2-(2-(1-(thiophen-2-yl)ethylidene)hydrazinyl)-5-(*p*-tolyl diazenyl)thiazole (**5b**) [72].

5-((4-Chlorophenyl)diazenyl)-4-methyl-2-(2-(1-(thiophen-2-yl)ethylidene)hydrazinyl)thiazole (**5c**) [72].

5-((4-Bromophenyl)diazenyl)-4-methyl-2-(2-(1-(thiophen-2-yl)ethylidene)hydrazinyl)thiazole (**5d**) [72].

4-Methyl-3-phenyl-5-(phenyldiazenyl)-2-((1-(thiophen-2-yl)ethylidene)hydrazineylidene)-2,3-dihydrothiazole (**5e**).

Red crystals; mp 191–193 °C (DMF); UV(DMSO):  $\lambda_{\max}$  = 385, 260 nm; IR (KBr)  $\nu_{\max}$ : 3036 (=C-H), 2925 (-C-H), 1601 (C=N)  $\text{cm}^{-1}$ ;  $^1\text{H-NMR}$  (DMSO- $d_6$ )  $\delta$ : 2.10 (s, 3H, CH<sub>3</sub>), 2.38 (s, 3H, CH<sub>3</sub>), 7.01–7.75 (m, 13H, ArH) ppm;  $^{13}\text{C-NMR}$  (100 MHz, DMSO- $d_6$ )  $\delta$ : 10.6, 16.0 (CH<sub>3</sub>), 110.7, 113.4, 116.1, 121.7, 121.9, 122.5, 124.3, 124.7, 126.3, 129.2, 131.5, 134.6, 138.6, 143.7, 152.5, 160.1 (Ar-C and C=N) ppm; MS  $m/z$  (%): 417 ( $M^+$ , 33). Anal. calcd for  $C_{22}H_{19}N_5S_2$  (417.11): C, 63.28; H, 4.59; N, 16.77; Found: C, 63.15; H, 4.38; N, 16.57%.

4-Methyl-3-phenyl-2-((1-(thiophen-2-yl)ethylidene)hydrazineylidene)-5-(*p*-tolyl diazenyl)-2,3-dihydrothiazole (**5f**).

Red crystals; mp 177–179 °C (EtOH); UV(DMSO):  $\lambda_{\max}$  = 376, 263 nm; IR (KBr)  $\nu_{\max}$ : 3048 (=C-H), 2920 (-C-H), 1600 (C=N)  $\text{cm}^{-1}$ ;  $^1\text{H-NMR}$  (DMSO- $d_6$ )  $\delta$ : 2.09 (s, 3H, CH<sub>3</sub>), 2.32 (s, 3H, CH<sub>3</sub>), 2.38 (s, 3H, CH<sub>3</sub>), 7.05–7.63 (m, 12H, ArH) ppm;  $^{13}\text{C-NMR}$  (100 MHz, DMSO- $d_6$ )  $\delta$ : 10.1, 14.8, 22.7 (CH<sub>3</sub>), 120.1, 125.3, 127.5, 127.8, 129.1, 129.3, 129.5, 130.0, 130.3, 134.5, 142.0, 143.2, 144.3, 147.7, 150.3, 161.9 (Ar-C and C=N) ppm; MS  $m/z$  (%): 431 ( $M^+$ , 100). Anal. Calcd. for  $C_{23}H_{21}N_5S_2$  (431.12): C, 64.01; H, 4.90; N, 16.23; Found: C, 63.85; H, 4.78; N, 16.08%.

5-(4-Methoxyphenyl)diazenyl)-4-methyl-3-phenyl-2-((1-(thiophen-2-yl)ethylidene)hydrazineylidene)-2,3-dihydrothiazole (**5g**).

Red crystals; mp 213–215 °C (DMF); UV(DMSO):  $\lambda_{\max}$  = 383, 263 nm; IR (KBr)  $\nu_{\max}$ : 3039 (=C-H), 2929 (-C-H), 1604 (C=N)  $\text{cm}^{-1}$ ;  $^1\text{H-NMR}$  (DMSO- $d_6$ )  $\delta$ : 2.09 (s, 3H, CH<sub>3</sub>), 2.38 (s, 3H, CH<sub>3</sub>), 3.79 (s, 3H, OCH<sub>3</sub>), 7.02–7.79 (m, 12H, Ar-H) ppm;  $^{13}\text{C-NMR}$  (100 MHz, DMSO- $d_6$ )  $\delta$ : 10.8, 16.1 (CH<sub>3</sub>), 56.1 (OCH<sub>3</sub>), 112.1, 115.9, 116.6, 120.8, 122.0, 122.6, 123.6, 125.7, 129.2, 132.1, 137.7, 138.3, 149.8, 150.7, 158.3, 161.2 (Ar-C and C=N) ppm; MS  $m/z$  (%): 447 ( $M^+$ , 29). Anal. Calcd. for  $C_{23}H_{21}N_5OS_2$  (447.12): C, 61.72; H, 4.73; N, 15.65; Found: C, 61.53; H, 4.86; N, 15.47%.

5-((4-Chlorophenyl)diazanyl)-4-methyl-3-phenyl-2-((1-(thiophen-2-yl)ethylidene)hydrazineylidene)-2,3-dihydrothiazole (**5h**).

Red crystals; mp 226–228 °C (DMF); UV(DMSO):  $\lambda_{\max}$  = 374, 266 nm; IR (KBr)  $\nu_{\max}$ : 3050 (=C-H), 2933 (-C-H), 1602 (C=N)  $\text{cm}^{-1}$ ;  $^1\text{H-NMR}$  (DMSO- $d_6$ )  $\delta$ : 2.10 (s, 3H, CH<sub>3</sub>), 2.38 (s, 3H, CH<sub>3</sub>), 7.13–7.68 (m, 12H, Ar-H) ppm;  $^{13}\text{C-NMR}$  (100 MHz, DMSO- $d_6$ )  $\delta$ : 10.2, 16.8, 22.7 (CH<sub>3</sub>), 119.1, 119.7, 126.1, 128.9, 129.3, 130.2, 130.8, 135.3, 135.5, 142.1, 147.6, 154.0, 154.4, 155.5, 158.8, 160.5 (Ar-C and C=N) ppm; MS  $m/z$  (%): MS  $m/z$  (%): 453 ( $\text{M}^+$ +2, 34), 451 ( $\text{M}^+$ , 10). Anal. Calcd. for C<sub>22</sub>H<sub>18</sub>ClN<sub>5</sub>S<sub>2</sub> (451.07): C, 58.46; H, 4.01; N, 15.49; Found: C, 58.37; H, 4.14; N, 15.35%.

3,5-Diphenyl-2-((1-(thiophen-2-yl)ethylidene)hydrazineylidene)-2,3-dihydro-1,3,4-thiadiazole (**7a**).

Yellow crystals; mp 201–203 °C (EtOH); UV(DMSO):  $\lambda_{\max}$  = 380, 258 nm; IR (KBr)  $\nu_{\max}$ : 3036 (=C-H), 2927 (-C-H), 1597 (C=N)  $\text{cm}^{-1}$ ;  $^1\text{H-NMR}$  (DMSO- $d_6$ )  $\delta$ : 2.15 (s, 3H, CH<sub>3</sub>), 6.91–8.05 (m, 13H, Ar-H) ppm;  $^{13}\text{C-NMR}$  (100 MHz, DMSO- $d_6$ )  $\delta$ : 15.8 (CH<sub>3</sub>), 116.9, 119.7, 121.4, 123.0, 123.6, 125.7, 126.2, 128.8, 130.4, 133.5, 137.4, 141.4, 149.5, 156.7, 160.3 (Ar-C and C=N) ppm; MS  $m/z$  (%): 376 ( $\text{M}^+$ , 54). Anal. Calcd for C<sub>20</sub>H<sub>16</sub>N<sub>4</sub>S<sub>2</sub> (376.08): C, 63.80; H, 4.28; N, 14.88. Found: C, 63.64; H, 4.19; N, 14.81%.

3-(4-Chlorophenyl)-5-phenyl-2-((1-(thiophen-2-yl)ethylidene)hydrazineylidene)-2,3-dihydro-1,3,4-thiadiazole (**7b**).

Yellow crystals; mp 219–221 °C (DMF); UV(DMSO):  $\lambda_{\max}$  = 332, 251 nm; IR (KBr)  $\nu_{\max}$ : 3036 (=C-H), 2927 (-C-H), 1597 (C=N)  $\text{cm}^{-1}$ ;  $^1\text{H-NMR}$  (DMSO- $d_6$ )  $\delta$ : 2.19 (s, 3H, CH<sub>3</sub>), 6.98–8.11 (m, 12H, Ar-H) ppm;  $^{13}\text{C-NMR}$  (100 MHz, DMSO- $d_6$ )  $\delta$ : 14.8 (CH<sub>3</sub>), 115.4, 115.6, 115.7, 121.8, 127.9, 128.0, 128.1, 128.3, 129.1, 129.4, 132.1, 137.8, 142.5, 149.8, 159.2, 161.5 (Ar-C and C=N) ppm; MS  $m/z$  (%): 410 ( $\text{M}^+$ , 39). Anal. Calcd for C<sub>20</sub>H<sub>15</sub>ClN<sub>4</sub>S<sub>2</sub> (410.04): C, 58.46; H, 3.68; N, 13.63. Found: C, 58.35; H, 3.57; N, 13.48%.

4-Phenyl-2-(2-(1-(thiophen-2-yl)ethylidene)hydrazineyl)thiazole (**9a**) [76].

4-(4-Methoxyphenyl)-2-(2-(1-(thiophen-2-yl)ethylidene)hydrazineyl)thiazole (**9b**) [77].

4-(3-Nitrophenyl)-2-(2-(1-(thiophen-2-yl)ethylidene)hydrazineyl)thiazole (**9c**) [76].

3,4-Diphenyl-2-((1-(thiophen-2-yl)ethylidene)hydrazineylidene)-2,3-dihydrothiazole (**9d**).

Brown crystals; mp 241–243 °C (DMF); UV(DMSO):  $\lambda_{\max}$  = 339, 254 nm; IR (KBr)  $\nu_{\max}$ : 3055 (=C-H), 2937 (-C-H), 1596 (C=N)  $\text{cm}^{-1}$ ;  $^1\text{H-NMR}$  (DMSO- $d_6$ )  $\delta$ : 2.14 (s, 3H, CH<sub>3</sub>), 6.58 (s, 1H, thiazole-H5), 7.01–7.57 (m, 14H, Ar-H) ppm;  $^{13}\text{C-NMR}$  (100 MHz, DMSO- $d_6$ )  $\delta$ : 16.1 (CH<sub>3</sub>), 110.2, 116.2, 118.9, 121.7, 122.8, 123.1, 123.9, 126.0, 127.4, 131.3, 135.9, 138.1, 144.6, 149.3, 153.7, 160.3 (Ar-C and C=N) ppm; MS  $m/z$  (%): 375 ( $\text{M}^+$ , 46). Anal. Calcd for C<sub>21</sub>H<sub>17</sub>N<sub>3</sub>S<sub>2</sub> (375.09): C, 67.17; H, 4.56; N, 11.19. Found: C, 67.04; H, 4.41; N, 11.13%.

3-Phenyl-2-((1-(thiophen-2-yl)ethylidene)hydrazineylidene)-4-(p-tolyl)-2,3-dihydrothiazole (**9e**).

Creamy microcrystals; mp 239–241 °C (DMF); UV(DMSO):  $\lambda_{\max}$  = 342, 259 nm; IR (KBr)  $\nu_{\max}$ : 3039 (=C-H), 2926 (-C-H), 1598 (C=N)  $\text{cm}^{-1}$ ;  $^1\text{H-NMR}$  (DMSO- $d_6$ )  $\delta$ : 2.12 (s, 3H, CH<sub>3</sub>), 2.18 (s, 3H, CH<sub>3</sub>), 6.51 (s, 1H, thiazole-H5), 7.00–7.49 (m, 13H, Ar-H) ppm;  $^{13}\text{C-NMR}$  (100 MHz, DMSO- $d_6$ )  $\delta$ : 14.5, 21.6 (CH<sub>3</sub>), 116.8, 117.3, 119.2, 126.0, 127.5, 128.6, 129.2, 130.2, 130.7, 138.6, 138.7, 142.1, 146.6, 152.5, 159.3, 162.4 (Ar-C and C=N) ppm; MS  $m/z$  (%): 389 ( $\text{M}^+$ , 46). Anal. Calcd for C<sub>22</sub>H<sub>19</sub>N<sub>3</sub>S<sub>2</sub> (389.10): C, 67.84; H, 4.92; N, 10.79. Found: C, 67.96; H, 4.82; N, 10.68%.

4-(4-Chlorophenyl)-3-phenyl-2-((1-(thiophen-2-yl)ethylidene)hydrazineylidene)-2,3-dihydrothiazole (**9f**).

Brown crystals; mp 250–252 °C (DMF); UV(DMSO):  $\lambda_{\max}$  = 328, 256 nm; IR (KBr)  $\nu_{\max}$ : 3044 (=C-H), 2930 (-C-H), 1599 (C=N)  $\text{cm}^{-1}$ ;  $^1\text{H-NMR}$  (DMSO- $d_6$ )  $\delta$ : 2.13 (s, 3H, CH<sub>3</sub>), 6.65 (s, 1H, thiazole-H5), 7.02–7.45 (m, 13H, Ar-H) ppm; MS  $m/z$  (%): 411 ( $\text{M}^+$ +2, 8), 409 ( $\text{M}^+$ , 27). Anal. Calcd for C<sub>21</sub>H<sub>16</sub>ClN<sub>3</sub>S<sub>2</sub> (409.05): C, 61.53; H, 3.93; N, 10.25. Found: C, 61.41; H, 3.83; N, 10.17%.

4-(4-Bromophenyl)-3-phenyl-2-((1-(thiophen-2-yl)ethylidene)hydrazineylidene)-2,3-dihydrothiazole (**9g**).

Brown crystals; UV(DMSO):  $\lambda_{\max}$  = 330, 248 nm; IR (KBr)  $\nu_{\max}$ : 3056 (=C-H), 2928 (-C-H), 1603 (C=N)  $\text{cm}^{-1}$ ;  $^1\text{H-NMR}$  (DMSO- $d_6$ )  $\delta$ : 2.10 (s, 3H,  $\text{CH}_3$ ), 6.65 (s, 1H, thiazole-H5), 7.01–7.49 (m, 13H, Ar-H) ppm;  $^{13}\text{C-NMR}$  (100 MHz, DMSO- $d_6$ )  $\delta$ : 14.8 ( $\text{CH}_3$ ), 109.0, 117.8, 120.9, 121.8, 122.1, 122.7, 122.9, 123.2, 126.0, 128.9, 134.7, 137.1, 137.7, 150.6, 159.9, 162.3 (Ar-C and C=N) ppm; MS  $m/z$  (%): 455 ( $\text{M}^+ + 2$ , 6), 453 ( $\text{M}^+$ , 19). Anal. Calcd for  $\text{C}_{21}\text{H}_{16}\text{BrN}_3\text{S}_2$  (453.00): C, 55.51; H, 3.55; N, 9.25. Found: C, 55.39; H, 3.40; N, 9.16%.

1-(4-Methyl-2-(2-(1-(thiophen-2-yl)ethylidene)hydrazineyl)thiazol-5-yl)ethan-1-one (**11a**) [76].

Ethyl 4-methyl-3-phenyl-2-((1-(thiophen-2-yl)ethylidene)hydrazineylidene)-2,3-dihydrothiazole-5-carboxylate (**11b**).

Yellow crystals; mp 180–182 °C (EtOH); UV(DMSO):  $\lambda_{\max}$  = 344, 257 nm; IR (KBr)  $\nu_{\max}$ : 3039 (=C-H), 29,224 (-C-H), 1723 (C=O), 1604 (C=N)  $\text{cm}^{-1}$ ;  $^1\text{H-NMR}$  (DMSO- $d_6$ )  $\delta$ : 1.24–1.27 (s, 3H,  $\text{CH}_2\text{CH}_3$ ), 2.04 (s, 3H,  $\text{CH}_3$ ), 2.17 (s, 3H,  $\text{CH}_3$ ), 4.20–4.23 (q, 2H,  $\text{CH}_2\text{CH}_3$ ), 6.81–7.53 (m, 8H, Ar-H) ppm;  $^{13}\text{C-NMR}$  (100 MHz, DMSO- $d_6$ )  $\delta$ : 12.1, 14.7, 14.8 ( $\text{CH}_3$ ), 61.1 ( $\text{CH}_2$ ), 96.4, 116.7, 120.1, 129.1, 129.4, 130.2, 142.0, 143.2, 144.2, 147.7, 153.3, 161.9 (Ar-C and C=N), 165.3 (C=O) ppm; MS  $m/z$  (%): 385 ( $\text{M}^+$ , 100). Anal. Calcd for  $\text{C}_{19}\text{H}_{19}\text{N}_3\text{O}_2\text{S}_2$  (385.09): C, 59.20; H, 4.97; N, 10.90. Found: C, 59.12; H, 4.79; N, 10.74%.

### 3.4. Docking Study

Ligand Preparation: Molecular operating environment software was used to carry out the molecular modeling for the most potent substances, which were sketched using Chemdraw 12.0. All minimizations were performed until a root mean square deviation (RMSD) gradient  $0.1 \text{ kcal} \cdot \text{mol}^{-1} \text{ \AA}^{-1}$  using MMFF 94 $\times$  (Merck molecular force field 94 $\times$ , Merck Research Laboratories, Rahway, NJ, USA).

### 3.5. Protein Preparation

The enzyme's X-ray crystal structure (PDB ID: 1JJJ, resolution: 3.20 Å) was downloaded in PDB format from the protein data bank [86]. The enzyme was prepared for docking studies: (i) hydrogen atoms were added to the structure with their standard geometry then reconnect the bonds broken and fixing the potential. (ii) Dummy atoms were constructed to the enzyme structure using the large site search in the enzyme structure; MOE alpha Site Finder is used [87]. (iii) In the protein's binding, pocket was marked. (iv) Analyzing the ligand's interaction with the active site's amino acids. Triangle Matcher placement method and London dG score tool were used for docking. After docking, both 2D and 3D interactions with amino acid residues were visualized. According to established protocols, all docking operations and scoring were documented [47,88,89].

## 4. Conclusions

Terephthalohydrazide chitosan hydrogel was prepared and characterized using FTIR, SEM, XRD, and TG analysis measurements. TCs was employed as a green heterogeneous basic catalyst for an efficient synthesis of very important bioactive thiazole and thiadiazole derivatives. The structures of all newly prepared products have been established on the basis of both spectroscopic data and elemental analysis. The results showed that TCs was a more effective heterogeneous basic catalyst in those processes than Cs, in addition to having a preferred green influence. The TCs catalyst was successfully reused three times with no appreciable decrease in catalytic efficiency when loaded at the appropriate rate of 10 wt%. As a result, this approach becomes greener and has more desirable qualities, such as being environmentally friendly, having a mild reaction condition, a short reaction time, excellent yields, and the capacity to recycle the catalyst. Finally, the TCs catalyst is a potential biopolymeric eco-friendly catalyst for future studies on various heterocyclic syntheses. Molecular docking in the active site of the *S. aureus* tyrosyl-tRNA synthetase revealed appropriate fitting with key residues in the active binding site with higher binding scores than the ligand in most. The detailed overview on the structure–activity relationship explained in the article will help the researchers to obtain a better understanding for

designing and developing novel antibacterial activity from thiazole moiety in the future. Finally, studies using ADME tools showed that thiazole moiety has drug-like properties. We hope that this paper will be highly informative to the scientific community engaged in discovering promising drug molecules to treat bacterial infections.

**Supplementary Materials:** The following supporting information can be downloaded at: <https://www.mdpi.com/article/10.3390/catal13091311/s1>, 2.1. Chemicals and Materials; 2.2. Measurements; the physical constants and analytical information for the known products **5a–d**, **9a–c**, and **11a** and some  $^1\text{H}$ -,  $^{13}\text{C}$ -NMR and Mass spectra of the synthesized compounds.

**Author Contributions:** J.Y.A.-H., S.M.G., N.A.A.E.-G., B.F., M.E.A.Z., T.Z.A. and N.A.M.: Supervision, Investigation, Methodology, Resources, Formal analysis, Data curation, Funding acquisition, Writing—original draft, Writing review and editing. All authors have read and agreed to the published version of the manuscript.

**Funding:** Princess Nourah bint Abdulrahman University Researchers Supporting Project number (PNURSP2023R24), Princess Nourah bint Abdulrahman University, Riyadh, Saudi Arabia.

**Data Availability Statement:** The data presented in this study are available on request.

**Conflicts of Interest:** The authors declare no conflict of interest.

## References

- Casti, F.; Basoccu, F.; Mocci, R.; Luca, L.D.; Porcheddu, A.; Cuccu, F. Appealing renewable materials in green chemistry. *Molecules* **2022**, *27*, 1988. [CrossRef] [PubMed]
- Macquarrie, D.J.; Hardy, J.J.E. Applications of Functionalized Chitosan in Catalysis. *Ind. Eng. Chem. Res.* **2005**, *44*, 8499–8520. [CrossRef]
- Guibal, E. Heterogeneous catalysis on chitosan-based materials: A review. *Prog. Polym. Sci.* **2005**, *30*, 71–109. [CrossRef]
- Kumar, M.N.V.R. A review of chitin and chitosan applications. *React. Funct. Polym.* **2000**, *46*, 1–27. [CrossRef]
- Toffey, A.; Samaranayake, G.; Frazier, C.E.; Glasser, W.G. Chitin derivatives. I. Kinetics of the heat-induced conversion of chitosan to chitin. *J. Appl. Polym. Sci.* **1996**, *60*, 75–85. [CrossRef]
- Sahu, P.K.; Sahu, P.K.; Gupta, S.K.; Agarwal, D.D. Chitosan: An efficient, reusable, and biodegradable catalyst for green synthesis of heterocycles. *Ind. Eng. Chem. Res.* **2014**, *53*, 2085–2091. [CrossRef]
- Ma, J.; Sahai, Y. Chitosan biopolymer for fuel cell applications. *Carbohydr. Polym.* **2013**, *92*, 955–975. [CrossRef]
- Elmehbad, N.Y.; Mohamed, N.A. Terephthalohydrazido cross-linked chitosan hydrogels: Synthesis, characterization and applications. *Int. J. Polym. Mater. Polym. Biomater.* **2022**, *71*, 969–982. [CrossRef]
- Mohamed, N.A.; Abd El-Ghany, N.A. Novel aminohydrazide cross-linked chitosan filled with multi-walled carbon nanotubes as antimicrobial agents. *Int. J. Biol. Macromol.* **2018**, *115*, 651–662. [CrossRef]
- Ablouh, E.; Hanani, Z.; Eladlani, N.; Rhazi, M.; Taourirte, M. Chitosan microspheres/sodium alginate hybrid beads: An efficient green adsorbent for heavy metals removal from aqueous solutions. *Sustain. Environ. Res.* **2019**, *29*, 5. [CrossRef]
- Pillai, C.K.S.; Paul, W.; Sharma, C.P. Chitin and chitosan polymers: Chemistry, solubility and fiber formation. *Prog. Polym. Sci.* **2009**, *34*, 641–678. [CrossRef]
- Mohamed, N.A.; Abd El-Ghany, N.A. Synthesis, characterization, and antimicrobial activity of chitosan hydrazide derivative. *Int. J. Polym. Mater. Polym. Biomater.* **2017**, *66*, 410–415. [CrossRef]
- Kumar, S.; Singhal, N.; Singh, R.K.; Gupta, P.; Singh, R.; Jain, S.L. Dual catalysis with magnetic chitosan: Direct synthesis of cyclic carbonates from olefins with carbon dioxide using isobutyraldehyde as the sacrificial reductant. *Dalton Trans.* **2015**, *44*, 11860–11866. [CrossRef] [PubMed]
- Dekamin, M.G.; Azimoshan, M.; Ramezani, L. Chitosan: A highly efficient renewable and recoverable bio-polymer catalyst for the expeditious synthesis of  $\alpha$ -amino nitriles and imines under mild conditions. *Green Chem.* **2013**, *15*, 811–820. [CrossRef]
- Baig, R.B.N.; Nadagouda, M.N.; Varma, R.S. Ruthenium on chitosan: A recyclable heterogeneous catalyst for aqueous hydration of nitriles to amides. *Green Chem.* **2014**, *16*, 2122. [CrossRef]
- Sun, J.; Wang, J.; Cheng, W.; Zhang, J.; Li, X.; Zhang, S.; She, Y. Chitosan functionalized ionic liquid as a recyclable biopolymer-supported catalyst for cycloaddition of  $\text{CO}_2$ . *Green Chem.* **2012**, *14*, 654–660. [CrossRef]
- Alshabanah, L.A.; Al-Mutabagani, L.A.; Gomha, S.M.; Ahmed, H.A. Three-component synthesis of some new coumarin derivatives as anti-cancer agents. *Front. Chem.* **2022**, *9*, 762248. [CrossRef]
- Gomha, S.M.; Riyadh, S.M.; Mahmmoud, E.A.; Elaasser, M.M. Synthesis and anticancer activities of thiazoles, 1,3-thiazines, and thiazolidine using chitosan-grafted-poly(vinylpyridine) as basic catalyst. *Heterocycles* **2015**, *91*, 1227–1243.
- Gomha, S.M.; Riyadh, S.M.; Mahmmoud, E.A.; Elaasser, M.M. Synthesis and anticancer activity of arylazothiazoles and 1,3,4-thiadiazoles using chitosan-grafted-poly(4-vinylpyridine) as a novel copolymer basic catalyst. *Chem. Heterocycl. Compd.* **2015**, *51*, 1030–1038. [CrossRef]



20. Alshabanah, L.A.; Gomha, S.M.; Al-Mutabagani, L.A.; Abolibda, T.Z.; Abd El-Ghany, N.A.; El-Enany, W.A.M.A.; El-Ziaty, A.K.; Ali, R.S.; Mohamed, N.A. Cross-linked chitosan/multi-walled carbon nanotubes composite as ecofriendly biocatalyst for synthesis of some novel benzil bis-thiazoles. *Polymers* **2021**, *13*, 1728. [\[CrossRef\]](#)
21. Xu, H.; Liao, W.M.; Li, H.F. A mild and efficient ultrasound-assisted synthesis of diaryl ethers without any catalyst. *Ultrason. Sonochem.* **2007**, *14*, 779–782. [\[CrossRef\]](#) [\[PubMed\]](#)
22. Cravotto, G.; Fokin, V.V.; Garella, D.; Binello, A.; Boffa, L.; Barge, A. Ultrasound-promoted copper-catalyzed azide-alkyne cycloaddition. *J. Comb. Chem.* **2010**, *12*, 13–15. [\[CrossRef\]](#)
23. Gomha, S.M.; Khalil, K.D. A Convenient ultrasound-promoted synthesis and cytotoxic activity of some new thiazole derivatives bearing a coumarin nucleus. *Molecules* **2012**, *17*, 9335–9347. [\[CrossRef\]](#) [\[PubMed\]](#)
24. Pizzuti, L.; Martins, P.L.G.; Ribeiro, B.A.; Quina, F.H.; Pinto, E.; Flores, A.F.C.; Venzke, D.; Pereira, C.M.P. Efficient sonochemical synthesis of novel 3,5-diaryl-4,5-dihydro-1H-pyrazole-1-carboximidamides. *Ultrason. Sonochem.* **2010**, *17*, 34–37. [\[CrossRef\]](#)
25. Ventola, C.L. The antibiotic resistance crisis: Part 1: Causes and threats. *Pharm. Ther.* **2015**, *40*, 277.
26. World Health Organization. *Antimicrobial Resistance: Global Report on Surveillance*; World Health Organization: Geneva, Switzerland, 2014.
27. PLoS Medicine Editors. Antimicrobial resistance: Is the world UNprepared? *PLoS Med.* **2016**, *13*, e1002130.
28. Solomon, S.L.; Oliver, K.B. Antibiotic resistance threats in the United States: Stepping back from the brink. *Am. Fam. Physician* **2014**, *89*, 938–941. [\[PubMed\]](#)
29. Cheesman, M.J.; Ilanko, A.; Blonk, B.; Cock, I.E. Developing new antimicrobial therapies: Are synergistic combinations of plant extracts/compounds with conventional antibiotics the solution. *Pharmacogn. Rev.* **2017**, *11*, 57–72.
30. Khan, S.; Iqbal, S.; Shah, M.; Rehman, W.; Hussain, R.; Rasheed, L.; Alrbyawi, H.; Dera, A.A.; Alahmdi, M.I.; Pashameah, R.A.; et al. Synthesis, in vitro anti-microbial analysis and molecular docking study of aliphatic hydrazide-based benzene sulphonamide derivatives as potent inhibitors of  $\alpha$ -glucosidase and urease. *Molecules* **2022**, *27*, 7129. [\[CrossRef\]](#)
31. Guo, M.; Gao, Y.; Xue, Y.; Liu, Y.; Zeng, X.; Cheng, Y.; Ma, J.; Wang, H.; Sun, J.; Wang, Z.; et al. Bacteriophage cocktails protect dairy cows against mastitis caused by drug resistant *Escherichia coli* infection. *Front. Cell. Infect. Microbiol.* **2021**, *11*, 690377. [\[CrossRef\]](#)
32. Faazil, S.; Malik, M.S.; Ahmed, S.A.; Jamal, Q.M.S.; Basha, S.T.; Al-Rooqi, M.M.; Obaid, R.J.; Qurban, J.; Shaikh, I.N.; Asghar, B.H.; et al. New quinoline-thiolactone conjugates as potential antitubercular and antibacterial agents. *J. Mol. Str.* **2023**, *1271*, 134099. [\[CrossRef\]](#)
33. Raimondi, M.V.; Presentato, A.; Li Petri, G.; Buttacavoli, M.; Ribaud, A.; De Caro, V.; Alduina, R.; Cancemi, P. New synthetic nitro-pyrrolomycins as promising antibacterial and anticancer agents. *Antibiotics* **2020**, *9*, 292. [\[CrossRef\]](#) [\[PubMed\]](#)
34. Raimondi, M.V.; Listro, R.; Cusimano, M.G.; La Franca, M.; Faddetta, T.; Gallo, G.; Schillaci, D.; Collina, S.; Leonchiks, A.; Barone, G. Pyrrolomycins as antimicrobial agents. Microwave-assisted organic synthesis and insights into their antimicrobial mechanism of action. *Bioorg. Med. Chem.* **2019**, *27*, 721–728. [\[CrossRef\]](#) [\[PubMed\]](#)
35. Spano, V.; Rocca, R.; Barreca, M.; Giallombardo, D.; Montalbano, A.; Carbone, A.; Raimondi, M.V.; Gaudio, E.; Bortolozzi, R.; Bai, R.; et al. Pyrrolo[2',3':3,4]cyclohepta[1,2-d][1,2]oxazoles, a New Class of Antimitotic Agents Active against Multiple Malignant Cell Types. *J. Med. Chem.* **2020**, *63*, 12023–12042. [\[CrossRef\]](#)
36. Cascioferro, S.; Maggio, B.; Raffa, D.; Raimondi, M.V.; Cusimano, M.G.; Schillaci, D.; Manachini, B.; Leonchiks, A.; Daidone, G. A new class of phenylhydrazinylidene derivatives as inhibitors of *Staphylococcus aureus* biofilm formation. *Med. Chem. Res.* **2016**, *25*, 870–878. [\[CrossRef\]](#)
37. Whatmore, J.L.; Swann, E.; Barraja, P.; Newsome, J.J.; Bunderson, M.; Beall, H.D.; Tooke, J.E.; Moody, C.J. Comparative study of isoflavone, quinoxaline and oxindole families of anti-angiogenic agents. *Angiogenesis* **2002**, *5*, 45–51. [\[CrossRef\]](#)
38. Jampilek, J. Heterocycles in Medicinal Chemistry. *Molecules* **2019**, *24*, 3839. [\[CrossRef\]](#) [\[PubMed\]](#)
39. Gomtsyan, A. Heterocycles in drugs and drug discovery. *Chem. Heterocycl. Comp.* **2012**, *48*, 7–10. [\[CrossRef\]](#)
40. Abdallah, A.E.; Mabrouk, R.R.; Al Ward, M.M.S.; Eissa, S.I.; Elkaeed, E.B.; Mehany, A.B.M.; Abo-Saif, M.A.; El-Feky, O.A.; Alesawy, M.S.; El-Zahabi, M.A. Synthesis, biological evaluation, and molecular docking of new series of antitumor and apoptosis inducers designed as VEGFR-2 inhibitors. *J. Enz. Inhib. Med. Chem.* **2022**, *37*, 573–591. [\[CrossRef\]](#)
41. Mohamed, H.A.; Ammar, Y.A.; Elhagali, G.A.M.; Eyada, H.A.; Aboul-Magd, D.S.; Ragab, A. In vitro antimicrobial evaluation, single-point resistance study, and radiosterilization of novel pyrazole incorporating thiazol-4-one/thiophene derivatives as dual DNA gyrase and DHFR inhibitors against MDR pathogens. *ACS Omega* **2022**, *7*, 4970–4990. [\[CrossRef\]](#)
42. Roman, G. Thiophene-containing compounds with antimicrobial activity. *Arch. Pharm Res.* **2022**, *355*, 2100462. [\[CrossRef\]](#) [\[PubMed\]](#)
43. Mabkhot, Y.N.; Kaal, N.A.; Alterary, S.; Mubarak, M.S.; Alsayari, A.; Bin Muhsinah, A. New thiophene derivatives as antimicrobial agents. *J. Heterocycl. Chem.* **2019**, *56*, 2845–2953. [\[CrossRef\]](#)
44. Wang, M.; Ma, J.; Wang, H.; Hu, F.; Sun, B.; Tan, T.; Li, M.; Huang, G. Brønsted acid-promoted ring-opening and annulation of thioamides and 2H-azirines to synthesize 2,4,5-trisubstituted thiazoles. *Org. Biomol. Chem.* **2023**, *21*, 5532–5536. [\[CrossRef\]](#) [\[PubMed\]](#)
45. Niu, Z.X.; Wang, Y.T.; Zhang, S.N.; Li, Y.; Chen, X.B.; Wang, S.Q.; Liu, H.M. Application and synthesis of thiazole ring in clinically approved drugs. *Eur. J. Med. Chem.* **2023**, *250*, 115172. [\[CrossRef\]](#) [\[PubMed\]](#)



46. Abouzied, A.S.; Al-Humaidi, J.Y.; Bazaid, A.S.; Qanash, H.; Binsaleh, N.K.; Alamri, A.; Ibrahim, S.M.; Gomha, S.M. Synthesis, Molecular Docking Study, and Cytotoxicity Evaluation of Some Novel 1,3,4-Thiadiazole as well as 1,3-Thiazole Derivatives Bearing a Pyridine Moiety. *Molecules* **2022**, *27*, 6368. [\[CrossRef\]](#) [\[PubMed\]](#)
47. Abdallah, A.M.; Gomha, S.M.; Zaki, M.E.A.; Abolibda, T.Z.; Kheder, N.A. A Green Synthesis, DFT calculations, and molecular docking study of some new indeno[2,1-b]quinoxalines containing thiazole moiety. *J. Mol. Str.* **2023**, *1292*, 136044. [\[CrossRef\]](#)
48. Anthwal, T.; Paliwal, S.; Nain, S. Diverse Biological Activities of 1,3,4-Thiadiazole Scaffold. *Chemistry* **2022**, *4*, 1654–1671. [\[CrossRef\]](#)
49. Krasavin, M. Novel 5-Nitrofuran-Tagged Imidazo-Fused Azines and Azoles Amenable by the Groebke-Blackburn-Bienaymé Multicomponent Reaction: Activity Profile against ESKAPE Pathogens and Mycobacteria. *Biomedicines* **2022**, *10*, 2203.
50. Lukin, A.; Komarova, K.; Vinogradova, L.; Rogacheva, E.; Kraeva, L.; Krasavin, M. Synthesis and Antibacterial Evaluation of Ciprofloxacin Congeners with Spirocyclic Amine Periphery. *Int. J. Mol. Sci.* **2023**, *24*, 954. [\[CrossRef\]](#)
51. Shetnev, A.; Tarasenko, M.; Kotlyarova, V.; Baykov, S.; Geyl, K.; Kasatkina, S.; Sibinčić, N.; Sharoyko, V.; Rogacheva, E.V.; Kraeva, L.A. External oxidant-free and transition metal-free synthesis of 5-amino-1,2,4-thiadiazoles as promising antibacterials against ESKAPE pathogen strains. *Mol. Divers.* **2023**, *27*, 651–666. [\[CrossRef\]](#)
52. Hu, J.; Su, Z.; Dong, B.; Wang, D.; Liu, X.; Meng, H.; Guo, Q.; Zhou, H. Characterization of a *Bacillus subtilis* S-16 Thiazole-Synthesis-Related Gene thiS Knockout and Antimicrobial Activity Analysis. *Curr. Issues Mol. Biol.* **2023**, *45*, 4600–4611. [\[CrossRef\]](#) [\[PubMed\]](#)
53. Wu, Z.; Shi, J.; Chen, J.; Hu, D.; Song, B. Design, Synthesis, Antibacterial Activity, and Mechanisms of Novel 1,3,4-Thiadiazole Derivatives Containing an Amide Moiety. *J. Agric. Food Chem.* **2021**, *69*, 8660–8670. [\[CrossRef\]](#)
54. King, D.E.; Malone, R.; Lilley, S.H. New classification and update on the quinolone antibiotics. *Am. Fam. Physician* **2000**, *61*, 2741–2748. [\[PubMed\]](#)
55. Abu-Melha, S.; Edrees, M.M.; Riyadh, S.M.; Abdelaziz, M.R.; Elfiky, A.A.; Gomha, S.M. Clean grinding technique: A facile synthesis and in silico antiviral activity of hydrazones, pyrazoles, and pyrazines bearing thiazole moiety against SARS-CoV-2 main protease (Mpro). *Molecules* **2020**, *25*, 4565. [\[CrossRef\]](#)
56. Khalil, K.D.; Riyadh, S.M.; Gomha, S.M.; Ali, I. Synthesis, characterization and application of copper oxide chitosan nanocomposite for green regioselective synthesis of [1,2,3]triazoles. *Int. J. Biol. Macromol.* **2019**, *130*, 928–937. [\[CrossRef\]](#) [\[PubMed\]](#)
57. Sayed, A.R.; Gomha, S.M.; Taher, E.A.; Muhammad, Z.A.; El-Seedi, H.R.; Gaber, H.M.; Ahmed, M.M. One-pot synthesis of novel thiazoles as potential anti-cancer agents. *Drug Des. Devel. Ther.* **2020**, *14*, 1363–1375. [\[CrossRef\]](#) [\[PubMed\]](#)
58. Gomha, S.M.; Riyadh, S.M.; Alharbi, R.A.K.; Zaki, M.E.A.; Abolibda, T.Z.; Farag, B. Green route synthesis and molecular docking of azines using cellulose sulfuric acid under microwave irradiation. *Crystals* **2023**, *13*, 260. [\[CrossRef\]](#)
59. Gomha, S.M.; Riyadh, S.M. Synthesis of triazolo[4,3-b][1,2,4,5]tetrazines and triazolo[3,4-b][1,3,4]thiadiazines using chitosan as ecofriendly catalyst under microwave irradiation. *Arkivoc* **2009**, *xi*, 58–68. [\[CrossRef\]](#)
60. Abu-Melha, S.; Gomha, S.M.; Abouzied, A.S.; Edrees, M.M.; Abo Dena, A.S.; Muhammad, Z.A. Microwave-assisted one pot three-component synthesis of novel bioactive thiazolyl-pyridazinediones as potential antimicrobial agents against antibiotic-resistant bacteria. *Molecules* **2021**, *26*, 4260. [\[CrossRef\]](#)
61. Gomha, S.M.; Abdalla, M.A.; Abdelaziz, M.; Serag, N. Eco-friendly one-pot synthesis and antiviral evaluation of pyrazolyl pyrazolines of medicinal interest. *Turk. J. Chem.* **2016**, *40*, 484–498. [\[CrossRef\]](#)
62. Gomha, S.M.; Edrees, M.M.; Muhammad, Z.A.; El-Reedy, M.A.A. 5-(Thiophen-2-yl)-1,3,4-thiadiazole derivatives: Synthesis, molecular docking and in-vitro cytotoxicity evaluation as potential anti-cancer agents. *Drug Des. Dev. Ther.* **2018**, *12*, 1511–1523. [\[CrossRef\]](#)
63. Aljohani, G.F.; Abolibda, T.Z.; Alhilal, M.; Al-Humaidi, J.Y.; Alhilal, S.; Ahmed, H.A.; Gomha, S.M. Novel thiadiazole-thiazole hybrids: Synthesis, molecular docking, and cytotoxicity evaluation against liver cancer cell lines. *J. Taibah Uni. Sci.* **2022**, *16*, 1005–1015. [\[CrossRef\]](#)
64. Abdalla, M.A.; Gomha, S.M.; Abdelaziz, M.R.; Serag, N. Synthesis and antiviral evaluation of some novel thiazoles and 1,3-thiazines substituted with pyrazole moiety against rabies virus. *Turk. J. Chem.* **2016**, *40*, 441–453. [\[CrossRef\]](#)
65. Alghamdi, A.; Abouzied, A.S.; Alamri, A.; Anwar, S.; Ansari, M.; Khadra, M.; Zaki, Y.H.; Gomha, S.M. Synthesis, Molecular Docking and Dynamic Simulation Tar-geting Main Protease (Mpro) of New Thiazole Clubbed Pyridine Scaffolds as Potential CoV-19 Inhibitors. *Curr. Issues Mol. Biol.* **2023**, *45*, 93. [\[CrossRef\]](#)
66. Gomha, S.M.; Muhammad, Z.A.; Abdel-aziz, M.R.; Abdel-aziz, H.M.; Gaber, H.M.; Elaasser, M.M. One pot synthesis of new thiadiazolyl-pyridines as anticancer and antioxidant agents. *J. Heterocycl. Chem.* **2018**, *55*, 530–536. [\[CrossRef\]](#)
67. Gomha, S.M.; Abdelhady, H.A.; Hassain, D.Z.H.; Abdelmonsef, A.H.; El-Naggar, M.; Elaasser, M.M.; Mahmoud, H.K. Thiazole based thiosemicarbazones: Synthesis, cytotoxicity evaluation and molecular docking study. *Drug Des. Dev. Ther.* **2021**, *15*, 659–677. [\[CrossRef\]](#) [\[PubMed\]](#)
68. Khalil, K.D.; Ahmed, H.A.; Bashal, A.H.; Bräse, S.; Nayl, A.; Gomha, S.M. Efficient, Recyclable, heterogeneous base nanocatalyst for thiazoles with chitosan capped calcium oxide nanocomposite. *Polymer* **2022**, *14*, 3347. [\[CrossRef\]](#)
69. Al-Ghamdi, R.F.; Fahmi, M.M.; Mohamed, N.A. Thermal stability and degradation behavior of novel wholly aromatic azopolyamide-hydrazides. *Polym. Degrad. Stab.* **2006**, *91*, 1530–1544. [\[CrossRef\]](#)
70. Mohamed, N.A. Biologically active maleimido aromatic 1,3,4-oxadiazole derivatives evaluated thermo-gravimetrically as stabilizers for rigid PVC. *J. Therm. Anal. Calorim.* **2018**, *131*, 2535–2546. [\[CrossRef\]](#)

71. Dessingiou, J.; Khedkar, J.K.; Rao, C.P. Chemosensing ability of hydroxynaphthylidene derivatives of hydrazine towards  $\text{Cu}^{2+}$ : Experimental and computational studies. *J. Chem. Sci.* **2014**, *126*, 1135–1141. [\[CrossRef\]](#)
72. Gomha, S.M.; Edrees, M.M.; Altalbawy, F.M.A. Synthesis and characterization of some new *bis*-pyrazolyl-thiazoles incorporating the thiophene moiety as potent anti-tumor agents. *Inter. J. Mol. Sci.* **2016**, *17*, 1499. [\[CrossRef\]](#) [\[PubMed\]](#)
73. Gomha, S.M.; Abdel-Aziz, H.A. Enaminones as building blocks in heterocyclic preparations: Synthesis of novel pyrazoles, pyrazolo[3,4-d]pyridazines, yrazolo[1,5-a]pyrimidines, pyrido[2,3-d]pyrimidines linked to imidazo[2,1-b]thiazole system. *Heterocycles* **2012**, *85*, 2291–2303. [\[CrossRef\]](#)
74. Shawali, A.S.; Harb, N.M.S.; Badahdah, K.O. A study of tautomerism in diazonium coupling products of 4-hydroxycoumarin. *J. Heterocycl. Chem.* **1985**, *22*, 1397–1403. [\[CrossRef\]](#)
75. Gomha, S.M. A facile one-pot synthesis of 6,7,8,9-tetrahydrobenzo[4,5]thieno[2,3-d]-1,2,4-triazolo[4,5-a]pyrimidin-5-ones. *Monatsh. Chem.* **2009**, *140*, 213–220. [\[CrossRef\]](#)
76. El-Naggar, A.M.; El-Hashash, M.A.; Elkaeed, E.B. Eco-friendly sequential *one-pot* synthesis, molecular docking, and anticancer evaluation of arylidene-hydrazinyl-thiazole derivatives as CDK2 inhibitors. *Bioorg. Chem.* **2021**, *108*, 104615. [\[CrossRef\]](#) [\[PubMed\]](#)
77. Chimenti, F.; Bizzarri, B.; Bolasco, A.; Secci, D.; Chimenti, P.; Granese, A.; Carradori, S.; D'Ascenzio, M.; Rivanera, D. Synthesis and biological evaluation of novel 2,4-disubstituted-1,3-thiazoles as anti-Candida spp. agents. *Eur. J. Med. Chem.* **2011**, *46*, 378–382. [\[CrossRef\]](#) [\[PubMed\]](#)
78. Alqurashi, R.M.; Farghaly, T.A.; Sabour, R.; Shaabana, M.R. Design, Synthesis, antimicrobial screening and molecular modeling of novel 6, 7 dimethylquinoxalin-2 (1H)-one and thiazole derivatives targeting DNA gyrase enzyme. *Bioorg. Chem.* **2023**, *134*, 106433. [\[CrossRef\]](#) [\[PubMed\]](#)
79. Bhat, A.A.; Tandon, N.; Singh, I.; Tandon, R. Structure-activity relationship (SAR) and antibacterial activity of pyrrolidine based hybrids: A review. *J. Mol. Str.* **2023**, *1283*, 135175. [\[CrossRef\]](#)
80. Yıldırım, M.; Çelikel, D.; Dürüst, Y.; Knight, D.W.; Kariuki, B.M. A rapid and efficient protocol for the synthesis of novel nitrothiazolo [3, 2-c] pyrimidines via microwave-mediated Mannich cyclisation. *Tetrahedron* **2014**, *70*, 2122–2128. [\[CrossRef\]](#)
81. Asgaonkar, K.; Tanksali, S.; Abhang, K.; Sagar, A. Development of optimized pyrimido-thiazole scaffold derivatives as anticancer and multitargeting tyrosine kinase inhibitors using computational studies. *J. Indian Chem. Soc.* **2023**, *100*, 100803. [\[CrossRef\]](#)
82. Alam, R.; Wahi, D.; Singh, R.; Sinha, D.; Tandon, V.; Grover, A. Design, synthesis, cytotoxicity, HuTopoII $\alpha$  inhibitory activity and molecular docking studies of pyrazole derivatives as potential anticancer agents. *Bioorg. Chem.* **2016**, *69*, 77–90. [\[CrossRef\]](#) [\[PubMed\]](#)
83. Daina, A.; Michielin, O.; Zoete, V. SwissADME: A free web tool to evaluate pharmacokinetics, drug-likeness and medicinal chemistry friendliness of small molecules. *Sci. Rep.* **2017**, *7*, 42717. [\[CrossRef\]](#)
84. Ragab, A.; Ammar, Y.A.; Ezzat, A.; Mahmoud, A.M.; Mohamed, M.B.I.; El-Tabl, A.S.; Farag, R.S. Synthesis, characterization, thermal properties, antimicrobial evaluation, ADMET study, and molecular docking simulation of new mono Cu (II) and Zn (II) complexes with 2-oxoindole derivatives. *Comput. Biol. Med.* **2022**, *145*, 105473. [\[CrossRef\]](#)
85. Mukhtar, S.S.; Morsy, N.M.; Hassan, A.S.; Hafez, T.S.; Hassaneen, H.M.; Saleh, F.M. A Review of Chalcones: Synthesis, Reactions, and Biological Importance. *Egypt. J. Chem.* **2022**, *65*, 379–395. [\[CrossRef\]](#)
86. Qiu, X.; Janson, C.A.; Smith, W.W.; Green, S.M.; McDevitt, P.; Johanson, K.; Carter, P.; Hibbs, M.; Lewis, C.; Chalker, A.; et al. Crystal structure of Staphylococcus aureus tyrosyl-tRNA synthetase in complex with a class of potent and specific inhibitors. *Protein Sci.* **2001**, *10*, 2008–2016. [\[CrossRef\]](#) [\[PubMed\]](#)
87. Labute, P. Protonate3D: Assignment of ionization states and hydrogen coordinates to macromolecular structures. *Proteins* **2009**, *75*, 187–205. [\[CrossRef\]](#)
88. Kattan, S.W.; Nafie, M.S.; Elmgeed, G.A.; Alelwani, W.; Badar, M.; Tantawy, M.A. Molecular docking, anti-proliferative activity and induction of apoptosis in human liver cancer cells treated with androstane derivatives: Implication of PI3K/AKT/mTOR pathway. *J. Steroid Biochem. Mol. Biol.* **2020**, *198*, 105604. [\[CrossRef\]](#) [\[PubMed\]](#)
89. Nafie, M.S.; Tantawy, M.A.; Elmgeed, G.A. Screening of different drug design tools to predict the mode of action of steroidal derivatives as anti-cancer agents. *Steroids* **2019**, *152*, 108485. [\[CrossRef\]](#) [\[PubMed\]](#)

**Disclaimer/Publisher's Note:** The statements, opinions and data contained in all publications are solely those of the individual author(s) and contributor(s) and not of MDPI and/or the editor(s). MDPI and/or the editor(s) disclaim responsibility for any injury to people or property resulting from any ideas, methods, instructions or products referred to in the content.